Protect or Prepare?

Crop Insurance and Adaptation in a Changing Climate*

Marguerite Obolensky†

March 2026

Abstract

As climate risks intensify, governments increasingly subsidize insurance against weather shocks. While these subsidies enhance short-run financial protection, they may dampen incentives for long-run adaptation to climate change. This paper studies how U.S. crop insurance subsidies shape agricultural adaptation. I develop and estimate a dynamic land-use model in which forward-looking farmers form beliefs about climate trends and make joint planting and insurance decisions under alternative subsidy regimes. Targeting subsidies toward regions with slower projected increases in climate risk partially mitigates the distortions created by the status quo by improving the spatial allocation of production. However, most gains come from decoupling subsidies from actuarially fair premiums, thereby restoring adaptation incentives.

*I am deeply indebted to Pietro Tebaldi, Gautam Gowrisankaran, Wolfram Schlenker, and Bernard Salanié for their invaluable help and support throughout this project. I would also like to thank Pierre Bodéré, Emma du Puy, Guillaume Fréchette, Myrto Kalouptsidi, Ashley Langer, Sebastián Otero, Maya Norman, Paul T. Scott, Andrey Simonov, Jeffrey Shrader, Isabella Smythe, Charles Taylor, and Roberto Zúñiga for many insightful comments and suggestions. I am grateful to Nahim Bin Zahur, Marshall Burke, and Ivan Ivanov for excellent discussions of the paper. Zachary White at the USDA Risk Management Agency and Chris Campbell at the Environmental Working Group provided helpful information on crop insurance subsidies. Any errors are my own.

†Kellogg School of Management, Northwestern University (marguerite.obolensky@gmail.com)

1 Introduction

Climate change is increasing exposure to extreme weather risk across a growing range of economic activities, from agriculture to infrastructure and manufacturing (Allan et al., 2023). Governments have responded by expanding subsidized insurance markets for households and firms (Kousky, 2019; OECD, 2021). While insurance improves short-run financial protection, it can also weaken incentives to adapt to shifting risk patterns (Kousky, 2019; Ferreira, 2024). The design of climate-risk insurance therefore faces a central trade-off: protecting current assets while preserving long-run adaptation incentives.

Agriculture is among the sectors most exposed to climate risk. In this paper, I study how the design of the U.S. Federal Crop Insurance Program shapes agricultural adaptation. The program accounts for roughly 30% of federal support to agriculture—about $5–$10 billion per year between 2010 and 2020—delivered primarily through premium subsidies. Because these subsidies are tied to actuarial risk, support tends to concentrate in high-risk regions and crops. This structure may slow adaptation by encouraging production of riskier crops and sustaining cultivation in increasingly vulnerable locations.

To quantify these forces, I develop and estimate a dynamic land-use model in which forward-looking farmers make joint planting and insurance decisions under evolving climate risk. The model combines crop insurance contract choice, weather-driven yield risk, and endogenous crop prices, so that subsidy design affects planting incentives by altering both expected revenues and revenue risk. I then combine the estimated model with climate projections to simulate equilibrium paths of land use and insurance choices under alternative subsidy designs between 2020 and 2050. I show that while status quo subsidies transfer income to farmers and increase insurance coverage, they also increase exposure to climate risk by encouraging production in riskier crops and locations. I then evaluate alternative subsidy designs that either target support based on projected climate-risk trends or decouple transfers from risk exposure altogether, and show that these reforms can improve on the status quo by reducing insurance-induced distortions while preserving income support.

I assemble detailed data on daily gridded weather, crop insurance contracts and premiums, land use from satellite imagery, and agricultural outcomes for the three main U.S. crops—corn, soybeans, and wheat. The data highlight three empirical patterns that the model must capture. First, climate projections indicate that exposure to extreme heat increases over time, and farmers face

greater uncertainty at planting about realized heat exposure over the growing season. Second, yields are sensitive to extreme heat—especially for corn and soybeans—yet the net yield impacts of climate change are spatially heterogeneous once changes in moderate temperatures and precipitation are taken into account, reshuffling comparative advantage across counties. Third, farmers adapt through crop switching, but rotations exhibit strong persistence, indicating meaningful adjustment frictions and rotation benefits.

The model has two stages. In the pre-planting season, the Risk Management Agency posts premiums and statutory premium subsidies for each crop–county–contract option.[1] Farmers observe these prices, past and current weather, and a low-dimensional aggregate market state summarizing national acreage. Based on these observations, they form beliefs on the upcoming growing season yields and prices. They then choose whether to plant corn, soybeans, or wheat, or leave land fallow. Conditional on planting, farmers select an insurance contract that trades off expected profits and revenue risk. During the growing season, weather realizes, and farmers harvest crops. Crop prices then result in equilibrium as a function of global production. Yields and prices jointly determine farmers' revenues and insurance payments.

Land-use decisions arise from a dynamic discrete choice problem. Current land use affects future choices because crop rotations generate agronomic complementarities and because switching entails adjustment costs (e.g., equipment changes, learning, or forming new trading partnerships). Farmers therefore trade off expected returns—net of subsidized insurance premiums, indemnities, and input costs—against rotation benefits or switching costs and discounted continuation values. A key feature of the state space is a parsimonious aggregate acreage state that summarizes national market conditions and determines crop prices. Following Krusell and Smith (1998) and Weintraub, Benkard, and Van Roy (2008), I assume atomistic farmers condition on this low-dimensional aggregate state rather than the full distribution of acreage across locations.

Crop insurance demand is modeled as a static discrete choice conditional on land use. Each option combines contract type (yield versus revenue protection) and coverage level. Revenue protection insures against both yield and price shocks, whereas yield protection insures against yield risk alone. Farmers choose among these options by trading off expected profits and revenue risk. For each contract, payoff distributions are evaluated using planting-time beliefs about weather, yields,

[1] Premiums are actuarially fair, so posted premiums adjust with expected indemnities, while subsidies follow the statutory schedule.

prices, and subsidized premiums in the upcoming growing season. Subsidy schedules therefore shift both insurance participation and the distribution of revenues, feeding back into planting incentives.

Estimation proceeds in two stages. First, I recover the planting-time belief objects that determine the payoff-relevant characteristics of insurance contracts and use them to estimate crop insurance demand. For yields, I infer risk from indemnity frequencies across coverage levels and map the recovered moments to pre-planting weather information. For prices, I discipline planting-time beliefs using pre-planting futures prices. Combining these belief objects with the RMA indemnity formulas and subsidy schedule yields expected revenues and revenue risk for each insurance option. I then estimate a static discrete-choice model of insurance demand using within-county–crop variation over time.

Second, I estimate the dynamic crop choice model by maximum likelihood using a nested fixed point algorithm. This stage requires constructing state-contingent payoff objects, including beliefs over yields and prices for aggregate acreage states not observed in the data and for future years through 2050. Because climate change makes the environment non-stationary, expected payoffs and continuation values vary over calendar time. I use the estimated insurance-demand system to map these beliefs into expected net returns under the optimal insurance choice and identify the dynamic parameters from cross-sectional and time-series variation in expected returns and in transition patterns across rotation histories.

The estimates imply economically meaningful risk aversion in insurance choices and substantial rotation-driven frictions in land use, with switching costs and rotation benefits on the order of hundreds of dollars per acre. These primitives discipline the model's counterfactual predictions for how subsidy design affects insurance take-up, crop switching, and equilibrium prices as climate risk evolves.

Under the status quo, subsidies provide meaningful short-run protection but distort adaptation incentives. Subsidies increase insurance participation and expand cultivated acreage, raising farmer surplus by about 1% relative to a no-subsidy benchmark. However, they also increase insured exposure—the amount of production whose downside risk is backed by the program—by nearly 6%. Because subsidies rise with actuarial risk, they encourage production in crops and locations that are increasingly vulnerable to climate shocks. These distortions worsen over time. In the model, costly crop switching slows the reallocation of land away from vulnerable production systems, so subsidy-induced misallocation compounds as climate risk evolves.

I then consider a simple forward-looking reform that varies subsidy generosity with projected regional climate-risk trends. This *By Region* policy reduces insured exposure while maintaining farmer surplus at the status quo level. By reallocating support away from counties where climate risk is projected to worsen most rapidly, the reform moderates the expansion of cultivated acreage and shifts production toward regions whose comparative advantage evolves more favorably under climate change.

However, targeting subsidies by region leaves an important distortion intact: because subsidies remain proportional to premiums, crops with higher actuarial risk still receive larger subsidy dollars within each county. As a result, the within-county tilt toward riskier crops persists. The largest reduction in insurance-induced distortions therefore arises when transfers are decoupled from actuarial risk altogether. Under this design, support continues to provide income protection to farmers but no longer rewards risk-taking production decisions.

Although adaptation can substantially reduce climate damages (IPCC, 2022; Costinot et al., 2016; Cui, 2020; Rising and Devineni, 2020), evidence on realized adaptation in agriculture remains mixed (Burke and Emerick, 2016; Hultgren et al., 2025). The literature has proposed several explanations for this incomplete adjustment, including technologies that are poorly suited to local agro-climatic conditions (Moscona and Sastry, 2025), financial frictions that discourage costly investment (Karlan et al., 2014), and limited climate information or forecasting capacity (Burlig et al., 2025). This paper studies another potential constraint on adaptation: when designed without climate trends in mind, agricultural policies, and in particular the U.S. Federal Crop Insurance Program, blunt private incentives to adjust as climate risks evolve.[2]

A growing literature shows that targeting environmental policy interventions increases environmental and welfare gains (Allcott et al., 2015; Duflo et al., 2018; Gerarden and Yang, 2023; Russo and Aspelund, 2024). In the context of climate change, related work emphasizes policies that explicitly promote adaptation, including mandated adaptation strategies and risk-based regulatory frameworks (Mach et al., 2019; Wagner, 2022; Baylis and Boomhower, 2026). I contribute to this

[2]Related work shows that public policies can weaken adaptation incentives in other settings; see, for example, Kousky et al. (2021); Fried (2022); Hsiao (2025); Druckenmiller et al. (2024); Baylis and Boomhower (2023). A large literature also studies the Federal Crop Insurance Program's effects on outcomes other than adaptation through crop switching, including production and land use (Nelson and Loehman, 1987; Goodwin et al., 2004; Walters et al., 2012; Claassen et al., 2017; Yu et al., 2018), input use (Smith and Goodwin, 1996; Mieno et al., 2018), irrigation (Deryugina and Konar, 2017; Suchato et al., 2022), productivity (Cornaggia, 2013), vulnerability to weather shocks (Annan and Schlenker, 2015), and yield variability (Wang et al., 2021). Among these papers, Annan and Schlenker (2015) is closest to my mechanism, showing that federal crop insurance increases yield sensitivity to extreme heat, potentially indicating that the program weakens adaptation incentives.

literature by showing that targeting regions with lower projected climate risk or decoupling transfers from risk exposure can improve on the Federal Crop Insurance Program status quo.

Finally, this paper contributes to two strands of empirical literature. First, it relates to work studying crop insurance demand and coverage choice. This literature examines how farmers choose among insurance products and coverage levels and how these choices respond to contract characteristics and subsidy design (Goodwin, 1993; Coble et al., 1996; Richards, 2000; Bulut et al., 2012; O'Donoghue, 2014; Ramirez and Shonkwiler, 2017; Tsiboe and Turner, 2023). My paper builds on this literature by estimating a structural demand system for crop insurance contracts that allows farmers to trade off expected revenues and revenue risk across coverage levels and contract types.

Second, the paper contributes to the literature that estimates dynamic models of land-use and crop-choice decisions. Recent work uses dynamic structural models to study farmers' responses to economic incentives and environmental conditions, including crop rotations, irrigation, and groundwater management (Scott, 2014; Dominguez-Iino, 2026; Burlig et al., 2026; Araujo et al., 2026). These models highlight the importance of adjustment costs and agronomic complementarities in shaping land-use persistence. I extend this framework by integrating crop insurance decisions into a dynamic crop-choice model with endogenous prices and evolving climate risk. This allows me to study how insurance policy design affects both insurance choices and long-run land-use adaptation.

2 Background on U.S. Crop Insurance

Farmland represents approximately 40% of the total contiguous U.S. area. Of these acres, 70% are planted with corn, soybeans, or wheat. Farmers must choose which crop to sow at the beginning of each calendar year,[3] with very little possibility of converting their decision by replanting in case of early crop failure.[4] This timeline makes planting decisions critical; these decisions must balance the benefits of crop rotations and expected prices and yields against input costs and risk.

Despite significant improvements in crop yields over the second half of the 20th century in the U.S., these remain sensitive to weather shocks. Temperatures exceeding 29–30° C (84–86° F) harm yields, particularly for corn and soybeans (Schlenker and Roberts, 2009; Gammans, Mérel, and Ortiz-Bobea, 2017). Therefore, a changing climate with increasing frequency of extreme heat

[3] One notable exception is winter wheat, which represents roughly 50% of wheat planted in my sample (Figure A1). Other wheat varieties are spring and durum, which follow corn and soybeans' planting/harvesting schedules. In the considered regions, winter wheat is planted in the fall and harvested a year later in August/September.

[4] In this paper, the growing season spans April to September, after which yields and revenues are realized.

events poses a significant risk to farmers' production and domestic agricultural output. During the worst year on record, 2012, half of the total crop losses nationwide were attributed to historical warming trends (Diffenbaugh, Davenport, and Burke, 2021).

To mitigate the (increasing) risks of uncertain yields and revenues, farmers can turn to crop insurance, offered to all farmers through a regulated, government-sponsored market. The Federal Crop Insurance Program was introduced in the 1930s as part of the New Deal following the droughts of the Dust Bowl and the Great Depression.[5] In 2010, 80% of American cropland was insured under the program, which represented 30% of the Farm Bill budget (between 5–10 billion USD per year between 2010 and 2020). Additionally, while 62% of farms producing row crops, such as corn, soybeans, and wheat, purchase federal crop insurance (Whitt, Lacy, and Lim, 2023), only around 25% of farmers are buying crop futures, options, or marketing contracts (MacDonald, 2020).

There are two main insurance contracts offered under the Multi-Peril Crop Insurance. Each available insurance product combines an insurance contract and a coverage level. Farmers who subscribe to a *yield protection* contract receive indemnities if their yields fall below a yield threshold—coverage levels times their historical yields—due to an environmental shock (drought, floods, extreme heat). Indemnity payments are the product of the yield shock (threshold minus realized yield) and the price of the crop future at the time of insurance subscription. *Revenue protection* contracts protect farmers against revenue loss due to either yield or crop price shocks.[6,7]

The Federal Crop Insurance Program is a public-private partnership. Farmers buy insurance policies from private insurers. The Risk Management Agency (RMA) acts as regulator and sponsor for the program. First, it mandates the types of insurance contracts that must be made available to farmers. Second, it determines farmers' premiums by setting subsidies and specific actuarial calculations. Third, the RMA supports private insurers by providing reinsurance and subsidies for their operating costs. These subsidies cover expenses such as monitoring compliance with RMA guidelines, including regulated planting dates, proper fertilization, pest control, and irrigation practices,

[5] More recently, the passage of the Federal Crop Insurance Reform Act in 1994 led to a spike in crop insurance subscriptions, reflecting the introduction of low-coverage, fully subsidized insurance and a temporary requirement that producers obtain insurance coverage to be eligible for other commodity support programs (Glauber, 2013). The Agricultural Risk Protection Act of 2000 increased crop insurance premium subsidies for plans with higher coverage.

[6] Farmers do not receive indemnities in a year where yields are low, but crop prices offset the loss of income. However, they are compensated in years when prices are low enough to pull their realized revenue below the guaranteed revenue threshold.

[7] Both *yield and revenue protection* are indemnity-based insurance. The USDA also started offering index-based insurance products around 2000, but these products are not as popular: together, yield and revenue protection account for 85% of the total policies sold (Congressional Research Service, 2021; Zulauf et al., 2020).

all aimed at reducing the risk of fraud and moral hazard.

The Federal government provides premium subsidies as a fixed share of insurance premiums, with subsidy rates varying by coverage level (see Appendix Table A1).[8] Premiums are based on a farmer's historical yields and harvest price projections and are set by the RMA to equal expected indemnities. Premiums are therefore exogenous to insurance choice, but vary systematically across locations, years, crops, and insurance contracts. In the model, I capture this variation parsimoniously as a function of local yield risk and crop prices (Section 4).

3 Data and Motivating Evidence

3.1 Data

Climate. I obtain historical gridded weather data from (PRISM Climate Group, 1985–2019). These data combine climate observations from a large monitoring network and climate models to produce spatially granular daily weather observations. In what follows, I use three county-level climate metrics: extreme degree days, growing degree days, and precipitation. Extreme (growing) degree days measure the exposure of a county to temperatures above 30°C (between 10 and 30°C).[9] For simulations in the future, I use weather projections from six climate models (Thrasher et al., 2016–2050) under a moderate (RCP4.5) emission scenario. During the main estimation period (2008–2019), U.S. counties experienced an average of 33 extreme degree days during the growing season (Table 1 panel A). However, extreme weather is spatially heterogeneous: the standard deviation of the number of extreme degree days is 1.3 times the average.

Land use. Land use data are obtained from a yearly land use classification of satellite imagery, the CropLand Data Layer (CDL) (Boryan et al., 2008–2021), available at a resolution of 30 meters. The CDL is produced using training and independent validation data from the Farm Service Agency Common Land Unit Program and the United States Geological Survey National Land Cover Database. The accuracy for crop-specific land cover ranges from 85% to 95%. These classifications are the basis for constructing transition probability between land covers (see Section 3.4 for details) and (area-weighted) county-level transition counts (see Section 5.2).

[8] These subsidies represent the largest share of total program costs; see https://www.ers.usda.gov/topics/farm-practices-management/risk-management/crop-insurance-at-a-glance.

[9] https://www.ers.usda.gov/data-products/chart-gallery/gallery/chart-detail/?chartId=108037

Table 1. Summary Statistics

Panel A: Climate	Mean	Median	Sd.
Extreme degree day (°C×day)	32.8	15.3	44.6
Growing degree day (°C×day)	1905.42	1865.38	437.28
Precipitation (mm)	683.4	678.5	188.6
Panel B: Insurance	Mean	Median	Sd.
Share insured	0.77	0.82	0.20
Average coverage (%)	57.7	61.6	15.5
Number of products	11.5	12.0	2.4
Paid premiums per acre	16.0	15.1	5.9
Subsidy per acre	26.8	24.7	11.1
Claim per acre	33.1	14.0	56.6
Panel C: Ag. Outcomes	Corn	Soybeans	Wheat
Yields (tons/acre)	3.94	1.28	1.32
Input Cost ($/ton)	166	126	75
Price ($/ton)	161	360	189
Production (million tons)	296	85	32
Exports (million tons)	44	38	15
Imports (million tons)	56	11	15
Fraction of U.S. ag. acres in sample	0.90	0.88	0.59

Notes: Panels A and B present county-level statistics computed for the sample of counties in Appendix Figure A1. Extreme degree days is the number of 30-degree days during the growing season, measured in °C×day. Total growing season precipitation is measured in mm. Both measures are obtained from PRISM for the period 2008-2020. Insurance data are obtained from the Risk Management Agency Summary of Business. Panel C presents crop-level averages of agricultural outcomes. Data were obtained from the U.S. Department of Agriculture National Agricultural Statistics Survey.

Crop insurance. County-crop-level information on insurance enrollment, paid premiums, and indemnities comes from the RMA Summary of Business database for the years 2011-2019 (RMA, 2023b). The Actuarial Information Browser provides data on premium pricing variables and formulas (RMA, 2023a). Corn, soybeans, and wheat growers in the sample insured close to 80% of their planted acres, at 60% coverage (Table 1 panel B). On average, 11.5 insurance products have a positive market share out of 16 products included in the study. Paid premiums are 16 dollars per acre on average. However, government premium subsidies during the study period are large: posted premiums are closer to $40 per acre (or between 7 and 15% of farmers' revenues), and farmers pay less than 40% of their premiums. Finally, farmers claim 32 dollars per acre on average, and the program is actuarially fair: realized claims per acre are equal to the share of insured acres times premiums per acre. However, claims are more volatile than premiums, suggesting that premiums do not account for correlated risks.

Agricultural outcomes. I obtain county-crop-level average yields and crop prices from the annual National Agricultural Statistics Survey (1985-2020), prices of agricultural futures from the Chicago Board of Trade (1975-2020), worldwide agricultural production and trade flows from FAO (2005–2020) and state-level input costs from the Agricultural Resource Management Survey (ARMS 1996–2020). U.S. corn yields are around 3.8 tons per acre, three times as large as soybeans and wheat yields (Table 1 panel C). Average crop prices differ sharply across commodities: soybeans command the highest price, around $360 per ton, compared to $161 for corn and $189 for wheat. Input costs also vary, with corn the most expensive to cultivate at about $166 per ton, followed by soybeans ($126) and wheat ($75). Sampled counties mainly produce corn: 296 million tons of corn are produced in these counties on average between 2008 and 2019, 15% of which are exported. Overall, my sample of U.S. counties produces about $51 billion of corn annually, compared with $30 billion of soybeans and $6 billion of wheat.

Sample restrictions. As in Schlenker et al. (2006), I focus on counties that follow relatively uniform agricultural practices, often referred to as "dry land farming" (Figure A1). For this I consider counties to the East of the 100th meridian West. Moreover, I exclude counties where farming is negligible (i.e. less than 5% of the surface is farmed), and among the remaining counties I study those in which corn, soybeans, and wheat production represents at least 60% of the planted area between 2008 and 2019. This allows me to study the transition between the three largest crops in the U.S. and how this interacts with climate change and crop insurance design. These cover 90% (60%) of total corn and soybeans (wheat) production nationwide (Table 1 panel C).

3.2 Climate Trends

Using projections from six global climate models under a moderate emission scenario, I estimate county-level trends in both the expected level and the uncertainty of extreme heat over 2020–2050. For each county-year, I compute the mean and standard deviation of growing-season extreme degree days implied by the projected distribution of growing-season weather.[10]

Figure 1 panel A shows the linear trend in extreme degree days. All counties in the sample experience an increase in extreme heat between 2020 and 2050, with half exhibiting a slope of at least one additional extreme degree day per year. This increase is of similar magnitude to baseline

[10]The distribution reflects uncertainty about growing-season weather (April–September) from the perspective of the pre-planting season (January–March). For each county-year, the climate projections imply a distribution of possible realizations of growing-season extreme degree days; the reported mean and standard deviation summarize this within-year predictive distribution

Figure 1. Trends in Extreme Degree Days



(A) Mean **(B)** Standard deviation

Notes: County-level linear trends estimated from six GCMs under RCP4.5, 2020–2050. Panel (a) measures hazard as the trend in the mean number of extreme degree days (>30°C). Panel (b) measures unpredictability as the trend in the standard deviation of extreme degree days. Slopes are reported in number of extreme degree day/year. See Appendix A4.1.1 for model and measurements details.

exposure in the sample (Table 1). Panel B shows the trend in the standard deviation of extreme degree days, capturing changes in within-year variability. All counties exhibit rising variability, indicating that planting-time forecasts of growing-season heat become increasingly uncertain over time.

Both maps reveal large geographic heterogeneity. Increases in extreme degree days are concentrated in the southern half of the sample, while unpredictability rises across much of the southern and central regions but remains relatively stable in parts of the North. These patterns are mirrored when looking at other measures of climate, such as the number of growing degree days and precipitation.

Together, these maps show that climate change increases both expected exposure to extreme heat and the uncertainty surrounding growing-season conditions. From the perspective of the pre-planting season, farmers face a higher mean and a wider distribution of extreme heat realizations, with substantial spatial heterogeneity across counties.

3.3 Extreme Temperatures and Yields

Weather shocks impact crop yields, and there is consensus that climate change will decrease the yields of most commodity crops in the future (Schlenker, Hanemann, and Fisher, 2006; Rising and Devineni, 2020; Hultgren et al., 2025). These effects are heterogeneous across crops, linking changes in weather to changes in relative crop profitability and, ultimately, in crop choice.

Table 2. Impact of Weather on Yields

Dependent Variable:	Log Yields		
Crop:	Corn	Soybeans	Wheat
	(1)	(2)	(3)
Extreme Degree Days	-0.0086***	-0.0064***	-0.0012*
	(0.0016)	(0.0007)	(0.0007)
County FE	Yes	Yes	Yes
State-Year FE	Yes	Yes	Yes
Observations	8,075	7,757	5,753
R^2	0.85	0.87	0.87

Notes: The sample includes all counties in Appendix Figure A1 between 2011 and 2019. Extreme degree days is the number of 30° C degree days measured during the growing season, expressed in tens. Wheat is a combination of winter and spring wheat. All specifications control for precipitation levels and the number of degree days between 10 and 30°. Standard errors are clustered at the state level. Significance levels: *** p<0.01, ** p<0.05, * p<0.1.

Leveraging year-to-year variation in the county-level weather during the growing season, I estimate, for each crop k:

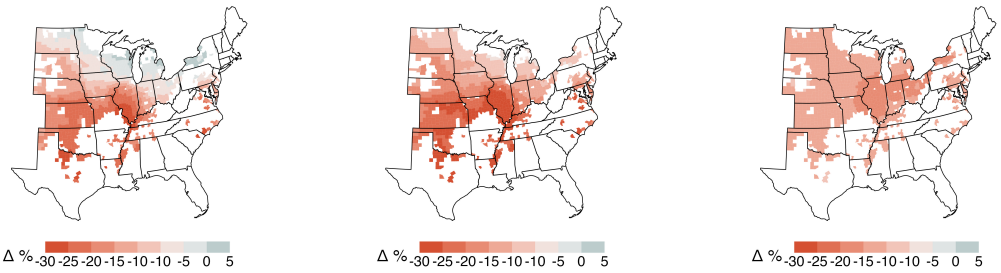
$$\ln \text{Yields}^k_{mt} = \beta^k \times \text{ExtremeDegreeDays}_{mt} + X_{mt} + \epsilon^k_{mt}, \tag{1}$$

where the dependent variable is the log of crop k yields in county m, in year t. The main variable on the right-hand side is the number of extreme degree days in county m, year t. X_{mt} includes county and state-by-year fixed effects, precipitation, and growing degree days.

Results are reported in Table 2. To keep the table readable, I report the coefficient on extreme degree days only. Consistent with prior evidence (see e.g. Schlenker and Roberts, 2009), ten additional extreme degree days during the corn (soybeans) growing season reduce yields by 8.6% (6.4%). The effect of extreme heat on wheat yields is smaller (-1.2%) and less precisely estimated, consistent with Gammans et al. (2017). Recent work suggests that the marginal effect of extreme heat may vary with baseline climate conditions (Jones et al., 2026). In Appendix Table A2, I allow the yield response to extreme degree days to differ between counties with above- and below-median baseline heat exposure. The estimated heat effects are broadly similar across county types, though soybean yields appear somewhat more sensitive in cooler counties.

While Table 2 isolates the marginal effect of extreme heat, climate change simultaneously alters moderate temperatures and precipitation. I combine the full set of estimated yield–weather relationships with projected changes in the three climate moments to compute net yield impacts

Figure 2. Change in realized yields 2020–2050



(A) Corn **(B)** Soybeans **(C)** Wheat

Notes: The maps show the spatial distribution of the projected percent change in county-level yields between 2015–2020 and 2045–2050. Climate evolves as projected by six general circulation models under a moderate emission scenario (see Section A4.1.1 for details). I average yearly yield projections across climate models.

between 2020 and 2050. Figure 2 shows that projected impacts are highly heterogeneous across space. Corn and soybeans experience large declines in many southern and central counties, but some northern counties see smaller losses or modest gains as increases in growing degree days partially offset heat damages. Wheat impacts are also mixed. Climate change therefore reshuffles comparative advantage across regions rather than uniformly favoring one crop.

In interpreting these findings one may be concerned about the confounding effect of moral hazard induced by the availability and prevalence of crop insurance. After insuring their crops, farmers could lower their productive effort to collect indemnities (Annan and Schlenker, 2015). Because insurance take-up is likely to be higher in locations more frequently exposed to severe weather shocks, this may bias estimates of the climate–yield relationship. (β^k) in Table 2. I address this issue in Appendix A1.2, where I exploit the 1994 reform, which resulted in a widespread but heterogenous increase in insurance take-up. Contrary to the moral hazard hypothesis, I do not find that yield responses to extreme degree days increase post-reform. I interpret this as evidence for a limited role of moral hazard, which may be consistent with the monitoring of insured farmers described in Section 2. In the remainder of the paper, I assume that insurance choices do not directly affect yields. I discuss the implications of this assumption in Section 4.3.

3.4 Crop Switching and Adaptation

As climate change increasingly threatens yields, farmers must adapt through various margins. Here, I focus on planting decisions, where farmers choose which crop to sow. Farming practices are also

subject to other adjustments, such as crop variety switching, that I do not consider in this paper.[11]

I construct two-lag conditional choice probabilities (CCPs) at the field level and then aggregate to the county level used in estimation. Construction proceeds in three steps. First, I resample the CDL to 600m × 600m (90 acres)[12] to reduce small-area misclassification. I keep four mutually exclusive land covers k: corn, soybeans, wheat, and fallow (pasture/cover/idle). For each pixel-year I build the lag labels (k_{t-1}, k_{t-2}) and merge time-invariant land quality θ, latitude/longitude, and year. Second, I estimate a pixel-level multinomial random forest that maps the state $(k_{t-2}, k_{t-1}, \theta, \text{lat}, \text{lon}, t)$ to the probability of each action k. This (i) avoids zero cells for sparse rotation histories, (ii) allows rich geographic and temporal heterogeneity, and (iii) nests simpler inverse-distance smoothers used in prior work (Scott, 2014; Araujo, Costa, and SantAnna, 2026; Burlig, Preonas, and Woerman, 2026). Third, I predict pixel-level CCPs and average within county to obtain $\widehat{\mathbb{P}}_{k'',k'\to k,mt}$.

Figure 3 reports average CCPs between 2011 and 2019. The matrix corroborates USDA reports in showing that crop switching is common (Wallander, 2013): farmers only engage in continuous cropping one-third of the time for wheat and about half of the time for corn and soybeans. Second, the corn-soybeans cycle dominates U.S. rotations: farmers who planted corn after soybeans (or soybeans after corn) continue the cycle with probabilities above 70%. This persistence underscores both the agronomic and economic benefits of rotation.[13] Third, transitions into or out of fallow are relatively rare. Farmers who idle a field for two years in a row choose to idle a third year with 92% probability, suggesting that the adjustment costs of re-entering are high. Conversely, once farmers are locked into continuous cultivation of corn, soybeans, wheat, or combinations of the three, they seldom fallow. This is consistent with the view that these decisions entail sunk investments and are path dependent. Finally, fallowing plays a nontrivial role in rotation strategies. The use of fallowing as a bridge is consistent with agronomic evidence that periods of uncultivated land can regenerate soil health and improve long-run productivity.[14]

Having established the existence of rotation patterns, I now examine whether medium-run climate shifts disrupt these choices and induce adaptation through crop switching. I compare the periods

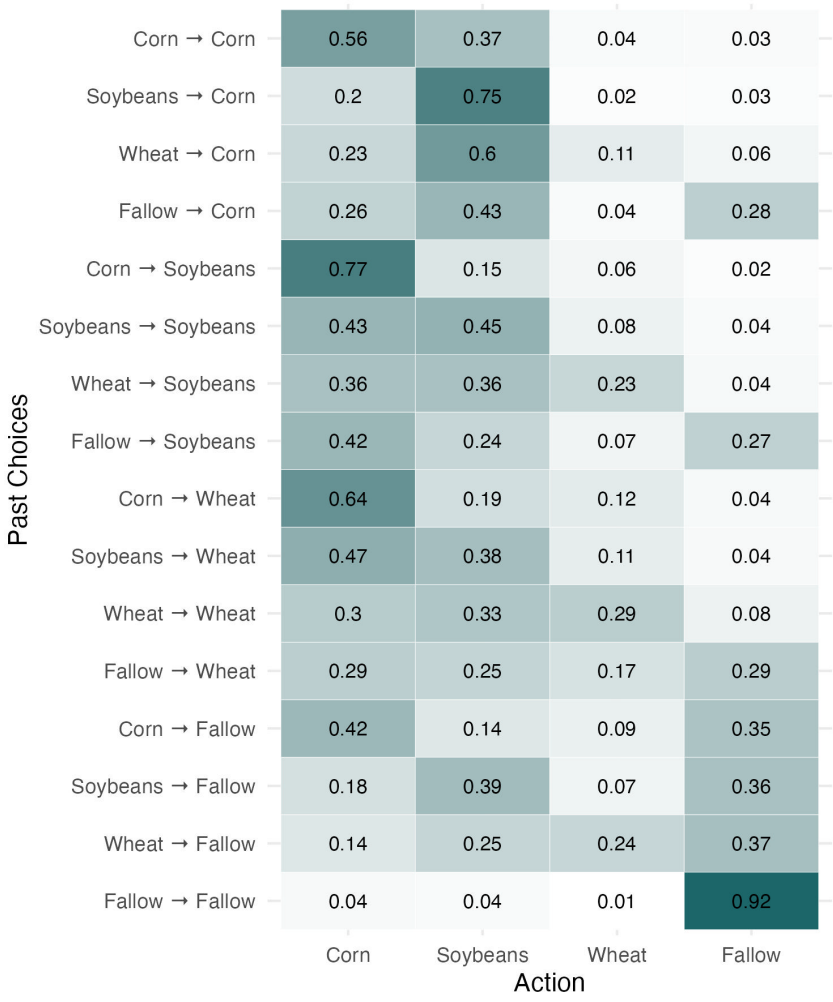
[11] Prior literature shows that this margin is somewhat limited, see, e.g., Burke and Emerick (2016).

[12] This is the median field area in the U.S. (Yan and Roy, 2016).

[13] The corn-soybeans sequence has been shown to deliver higher yields and reduced fertilizer requirements (Al-Kaisi et al., 2015; Bakhsh and Kanwar, 2007; Sindelar et al., 2015).

[14] See, e.g., Ruis et al. (2023); Peng et al. (2024) for recent evidence on the soil-regenerative benefits of alternating active cropping with fallowing.

Figure 3. Conditional Choice Probabilities



Notes: Each cell reports the probability of planting a given crop (columns) conditional on the previous two years' crops (rows). The sample of counties included in the analysis is shown in Figure A1.

2011–2014 to 2016–2019 and regress changes in average CCPs on changes in extreme degree days, precipitation, and growing degree days. For exposition, I focus on extreme degree days, interpreting the coefficients as the partial effect of rising extreme heat holding other weather shifts fixed. For each triple of crop k'', k', k, and each county m, I estimate

$$\Delta_t \mathbb{P}_{k'',k' \to k,m} = \beta \times \Delta_t \text{ExtremeDegreeDays}_m + \Delta_t X_m + \Delta_t \varepsilon_{k'',k',k,m}. \tag{2}$$

Figure A3 reports how trends in exposure to extreme heat affect farmers' crop switching decisions. Holding changes in precipitation and growing degree days fixed, the coefficients reveal a clear pattern: increases in extreme degree days reduce the likelihood of maintaining or switching into

corn and soybeans, while the corresponding effects for wheat and fallow are generally positive. These findings are consistent with the heat-sensitivity patterns in Table 2 and indicate that, holding other weather shifts fixed, farmers respond to rising extreme heat by reallocating land away from heat-sensitive crops toward more heat-tolerant crops or idling land.

Quantitatively, the median estimate by crop implies that ten additional extreme degree days reduce the probability of planting corn (soybeans) by about 1.5 (1.1) percentage points, while increasing the probability of planting wheat (fallow) by 1.0 (1.4) percentage points. To translate these magnitudes into meaningful units, I simulate the effect of an homogeneous increase of ten additional extreme degree days on agricultural acreage (Figure A4). Such a change leads to a 2.5 percent reduction in corn acreage (about 2.1 million acres) and a 2.5 percent decline in soybean acreage (1.5 million acres), offset by an 8.5 percent increase in wheat coverage (1.4 million acres) and a 2.5 percent rise in fallow land (2.2 million acres).

These results suggest that crop switching is a viable adaptation margin to warming trends: farmers re-optimize rotations in response to changes in climatic conditions. However, quantifying how crop insurance subsidies distort these adaptive responses requires an equilibrium framework. The next section develops a structural model that incorporates the full evolution of weather risk and the crop insurance system to quantify how subsidy design shapes adaptation under climate change.

4 Empirical Model

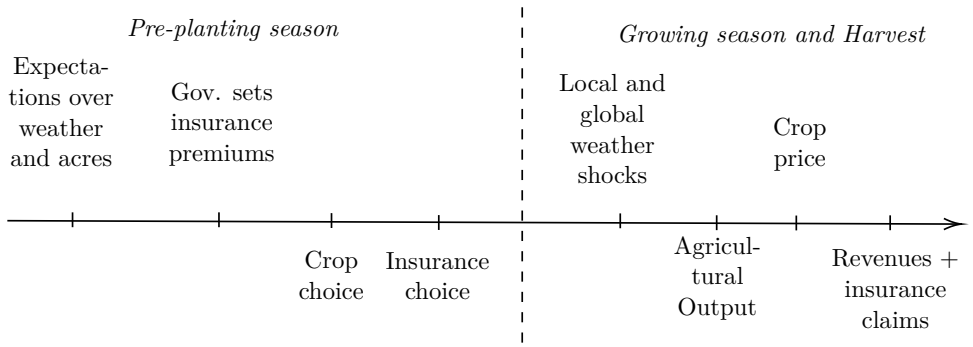
4.1 Overview

The model is composed of two blocks: a pre-planting period during which all farmers' decisions take place and a growing and harvest season during which production, prices, and profits are realized. The timeline is illustrated in Figure 4.

During the pre-planting season, farmers observe subsidized crop insurance premiums and form beliefs about (*i*) local weather shocks, (*ii*) weather shocks in other counties and abroad, and (*iii*) planted acres of each crop in the U.S. and abroad. Together, beliefs over these variables lead farmers to form beliefs over their individual production, as well as U.S. and foreign production. These ultimately result in beliefs over growing season revenues across alternative planting decisions. Farmers then make a land use decision, followed by a crop insurance decision.[15] Throughout my

[15]Insurance choice follows planting decisions insofar farmers do not grow seeds from their own production (to avoid

Figure 4. Timing of Farmers' Decisions



analysis, farmers are atomistic and farmers' decisions are modeled independently across monocultured fields.[16] After planting and insurance decisions are made, weather shocks, yields, prices, insurance indemnities, and profits realize.

4.2 Econometric Specification

I specify the primitives and distributional assumptions of the model proceeding backward along the timeline illustrated in Figure 4.

4.2.1 Growing Season and Harvest

During the growing season, local and global weather shocks realize. Given the land use decisions inherited from the pre-planting season, these shocks affect aggregate agricultural production. For the U.S., the total production of crop k in year t is

$$Q_t^{k,US} = \sum_{i \in US} \mathbf{1}\{\text{Farmer } i \text{ chooses } k\} \text{Yields}_{it}^k(\text{Weather}_{it}^{GS}) \tag{3}$$

where Weather_{it}^{GS} is the growing season weather experienced by farmer i in county m_i in year t.

Crop prices equilibrate aggregate supply and demand. Rather than imposing a fully specified demand-and-trade structure, I model the price response to supply shifts using a reduced-form inverse-demand relationship estimated by weather-based IV. Specifically, for crop k and year t, log

cross-pollination and ensure the best performance possible). Instead, they buy seeds 2-3 months before the planting season (see this Center for Arkansas Farm and Food System article). In contrast, farmers typically meet with a crop insurance agent the month before the regulated planting date (see this article on important crop insurance dates).

[16] First, it follows that farmers are price-takers. This assumption is common, and plausible given that agricultural commodity markets are highly integrated and that one agricultural field performance has a negligible effect on aggregate variables. Second, the independence assumption rules out risk hedging between fields. I discuss the implications of the omission of scale effects in Section 4.3.

U.S. prices satisfy

$$\ln p_t^k = \beta_k + \beta_Q \ln Q_{kt} + \nu_{kt}, \tag{4}$$

where Q_{kt} is total production (U.S. plus rest-of-world) and β_k are crop fixed effects. Identification relies on growing-season weather shocks as instruments for $\ln Q_{kt}$, capturing plausibly exogenous shifts in supply.[17] Given the price p_t^k and realized yields, the static profits of a farmer i who planted k and selected crop insurance option j are equal to

$$R_{ijt}^k = \underbrace{p_t^k \times \text{Yields}_{it}^k(\text{Weather}_{it}^{GS}) - \text{InputCosts}_{it}^k}_{\text{Profits from crop sale}} + \underbrace{\text{Indemnity}_j^k\left(\text{Yields}_{it}^k(\text{Weather}_{it}^{GS}), p_t^k\right) - \text{SubsPremium}_{ijt}^k}_{\text{Revenues from crop insurance}}. \tag{5}$$

4.2.2 Crop Insurance Demand

In the last stage of the pre-planting season, given crop choice k, farmer i must choose one insurance option $j \in \mathcal{J}$, or remain uninsured ($j = 0$). Each insurance contract combines one of the two types of coverage (revenue or yield; cf. Section 2) with one of eight coverage levels (50% to 85%). The type determines whether indemnities are triggered by yield shocks alone or by both yield and price shocks, while the coverage level dictates the generosity of the payout schedule.

A farmer is characterized by their county m. For insurance product j and crop k, farmer i's weather and aggregate production beliefs are such that the distribution of static profits have mean and variance equal to, respectively

$$\mathbb{E}_{jtm}^k \equiv \mathbb{E}\left[R_{ijt}^k \middle| m\right], \quad \text{and} \quad \text{Var}_{jtm}^k \equiv \text{Var}\left[R_{ijt}^k \middle| m\right].$$

I assume farmers have constant absolute risk aversion (CARA) preferences and that static profits are approximately normally distributed. The indirect utility for farmer i who planted crop k in

[17] Appendix A2 documents the estimation of (4) and shows robustness to crop-specific elasticities and to using U.S. production only. This price block delivers a stable, data-consistent mapping from domestic and foreign production shocks into the U.S. prices that enter realized revenues and insurance indemnities. A more structural alternative would be to calibrate a demand-and-trade system. Results in Section 6 are qualitatively similar when replacing (4) with a parsimonious CES demand specification in the spirit of Costinot et al. (2016) (not shown).

county m when selecting insurance j is

$$u_{ijt} = \beta^E \Delta\mathbb{E}^k_{jtm} - \beta^V \Delta Var^k_{jtm} + \xi^k_{jtm} + \varepsilon_{ijt}, \tag{6}$$

where $\Delta\mathbb{E}^k_{jtm} = \mathbb{E}^k_{jtm} - \mathbb{E}^k_{0tm}$ and $\Delta Var^k_{jtm} = Var^k_{jtm} - Var^k_{0tm}$. ε_{ijt} is i.i.d. type 1 extreme value and the unobservable determinants of demand for insurance j are collected in ξ^k_{jtm}. The utility derived from choosing the outside option is $u_{i0t} = \varepsilon_{i0t}$.[18]

To make the planting decisions modeled next, farmers do not yet know the realizations of the idiosyncratic preference shocks ε^k_{ijt}, but have rational expectations about their future optimal crop-insurance choice. That is, they know that if they select crop k, the expected total net static profits are

$$\mathbb{E}^*_{kmt} = \mathbb{E}^k_{0tm} + \frac{u^*_{kmt}}{\beta^E} = \mathbb{E}^k_{0tm} + \frac{\ln \sum_j \exp(u_{ijt} - \varepsilon_{ijt})}{\beta^E}. \tag{7}$$

4.2.3 Dynamic Crop Choice

During the pre-planting season, farmer i must choose among four possible, mutually exclusive land uses $k \in \mathcal{K} = \{\text{corn, soybeans, wheat, fallow}\}$.[19] This choice is dynamic because planting k affects not only expected profits in the current year but also future payoffs through history-dependent effects.

Specifically, at the beginning of year t crop choice must take into account the vector of state variables, which follows a first-order Markov process and contains the farmer's two-lag land use history, local weather shocks, weather shocks in other counties and abroad, aggregate acreage planted for each crop in the U.S. and abroad, crop insurance subsidies, input costs, and k-specific idiosyncratic shocks ϵ_{ikt}.[20] As is common, I assume the state space joint density function is conditionally independent and that ϵ_{ikt} is i.i.d type 1 extreme value. The state space can be summarized by a farmer i's past land use choices k'', k', their county m, the calendar year t, and a discrete aggregate acreage state s that summarizes national planted acres (and therefore pins down crop prices; see

[18] Under CARA preferences with normally distributed profits, expected utility can be written as $\mathbb{E}[U(\pi)] \approx \mathbb{E}[\pi] - \lambda/2 Var(\pi)$, where λ is the coefficient of constant absolute risk aversion. This implies $\lambda = -2\beta^V/\beta^E$. In what follows, I will also report the relative risk aversion evaluated at the outside-option per-acre mean static profits: $\lambda\mathbb{E}_0$.

[19] In practice, fallow corresponds to one of the following: pasture, cover crops, and fallow. I exclude other crops, forests and built areas from the analysis.

[20] This simplified state space—instead of tracking all cultivated acres in every county, farmers track U.S. aggregated acres in the spirit of Krusell and Smith (1998) and Weintraub et al. (2008)—makes the problem computationally tractable.

Appendix A2 for details).

Farmer i realizes per-period payoffs that depend on the choice k equal to

$$\pi_{k'',k'\to k,imt} = \phi_{k'',k'\to k} + \alpha \mathbb{E}^*_{kmt}(s) + \epsilon_{ikt}. \tag{8}$$

The history-dependent term $\phi_{k'',k'\to k}$ depend on the planting decisions made in the past two year ($k_{t-1} = k', k_{t-2} = k''$) and average to 0 by land cover k. They capture both agronomic complementarities (e.g., yield gains from rotations, pest suppression) and adjustment frictions (e.g., equipment setup, learning-by-doing), and are the main drivers of path dependence in land use. $\mathbb{E}^*_{kmt}$ are expected net static profits, defined in Equation (7) and function of the aggregate acres s through their dependence on crop prices. α capture the elasticity of the flow payoffs with respect to the static profits.[21]

By the Bellman's principle of optimality,

$$V_{k'',k',imts} = \max_{k\in\mathcal{K}} \{\pi_{k'',k'\to k,imt} + \delta\, \mathbb{E}[V(_{k',k,imt+1s'}|\ k, k'', k', i, m, t, s]\ \}, \tag{9}$$

where $V_{k'',k',imts}$ is the expected discounted stream of profits under optimal behavior. The discount factor δ is treated as known and equal to 0.9.

4.3 Discussion

Throughout the analysis, I assume that farmers make independent insurance and land use decisions across fields. The following factors attenuate the concern that this approach may omit scale effects in planting and insurance choices.[22] First, larger farms tend to be spatially concentrated (see Appendix Figure A10). I estimate the crop insurance demand model using within-county variation which should partly capture farm size heterogeneity. In robustness analyses, I show that estimates are not driven by counties with a high share of small farms. Second, the literature (see e.g.

[21] As in standard multinomial logit models, utility coefficients are identified only up to scale. Throughout, I adopt the usual normalization $\sigma_\epsilon = 1$, implying that α should be interpreted as responsiveness to expected profits relative to the dispersion of idiosyncratic shocks. Ratios such as ϕ/α are invariant to this normalization and admit a money-metric interpretation.

[22] Concern is that large farms may have greater access to alternative risk-hedging solutions such as futures and options markets or diversifying their crop mix over multiple fields. Omission of scale effects may result in underestimating farmers' distaste for revenue risk and overestimating premium sensitivity—thus leading to inflated impacts of crop insurance subsidies on the agricultural system. Additionally, observed low crop switching probability is rationalized by larger switching costs when it could be explained by portfolio diversification.

MacDonald, 2020) suggests that farmers see their various risk-hedging options as complements, limiting the concern that other risk-hedging solutions influence their crop insurance choice.

As discussed in Section 3.3, the analysis abstracts from moral hazard and treats yield distributions as independent of farmers' insurance choices. If effort responses were substantial (in contradiction to what I find in Appendix Section A1.2), insured yields would be endogenously lower and more variable, and the current approach would mis-measure the mean and variance objects entering the insurance and crop choice models. In that case, the estimated sensitivities to expected returns and risk ($\beta^{\mathbb{E}}$ and β^{V}) and the dynamic response to profit changes (α) would all be biased downward. Counterfactual simulations would understate both the risk-smoothing value of coverage for farmers and the behavioral distortions induced by subsidies, with ambiguous implications.

Margins of adaptation other than crop switching are not explicitly modeled in this analysis. For example, I focus my empirical sample on agricultural land east of the 100th meridian, which is overwhelmingly rainfed and not heavily reliant on irrigation infrastructure (Schlenker et al., 2006), and rule out large-scale shifts into irrigation as a hedge against climate risk. Equilibrium impacts of this omission are ambiguous. The presence of generous subsidies may reduce farmers' incentive to switch to or expand irrigation. At the same time, subsidies could increase total water withdrawals through reallocation toward more water-intensive crops (Deryugina and Konar, 2017).

Likewise, I abstract from the possibility of adopting drought- or heat-resistant seed varieties. While genetically engineered crops such as herbicide-tolerant and insect-resistant varieties have achieved near-universal adoption in major U.S. crops, the adoption of drought-resistant corn seeds remains modest at about 20% (McFadden et al., 2019). By excluding this margin of adaptation, the paper likely understates the costs of reduced innovation or slower adoption of climate-resilient seeds that may be discouraged by an insurance regime that dampens farmers' risk incentives.

In the model, farmers are treated as renters rather than landowners: rental prices enter revenues via input costs in Equation (5). I abstract from the capitalization of crop-insurance subsidies into rental or land prices. Empirical evidence suggests that a share of subsidy benefits are passed through to landowners via higher cash rents or land values (e.g., Kirwan, 2009). Accounting for land-market capitalization would likely lower the estimated producer surplus gains and attenuate the distortionary effects of the subsidies.

Finally, I assume farmers (and the government) have rational beliefs on climate change. If, instead,

I assumed farmers did not expect climate change, I would estimate larger switching costs: farmers would expect future yields to be higher than they are, yet I observe low crop switching probabilities. The resulting higher switching costs would reinforce path dependency, increasing the likelihood that crop insurance subsidies could lock the U.S. agricultural system into a low-adaptation trajectory.

5 Estimation

5.1 Crop Insurance Demand

Short-run beliefs and insurance characteristics. For each insurance option j, I construct farmers' planting-time beliefs about agricultural revenues. These beliefs are determined by two underlying distributions—crop-county-year yields and crop-year prices—and are treated as exogenous to farmers' insurance and land-use decisions. In particular, yields do not depend on insurance take-up (as discussed in Section 3.3) and farmers are price-takers.

Yield beliefs are constructed in two steps (Appendix A2). First, I recover county-level yield distributions from administrative crop insurance data for 2011–2019. Indemnity frequencies at different coverage levels identify lower-tail probabilities. Assuming yields are lognormal and centered on the USDA county-year mean, I infer yield variance using a Bayesian binomial-likelihood procedure. Second, I relate the recovered yield moments to growing-season weather conditions (extending Equation 1) and estimate weather-forecasting models that map pre-planting information into planting-time beliefs. Simulating these forecasts through the yield models delivers county–crop–year beliefs about the full yield distribution. Beliefs about crop prices are derived from pre-planting futures prices using a quantile random forest model. Combining yield and price beliefs with insurance contract design yields expected revenues $\mathbb{E}^k_{jtm}$ and revenue risk Var^k_{jtm} for each insurance option.

To measure premiums consistently across all contracts—including those not purchased in a county—I compute actuarially fair premiums using the estimated yield and price distributions and apply the statutory subsidy schedule in Table A1. This procedure implies that farmers and the RMA share the same beliefs about growing-season outcomes, so premiums do not convey additional information about local yields or prices.

Table 3 reports the resulting insurance characteristics. Expected revenues $\mathbb{E}^k_{jtm}$ (net of subsidized premiums) increase with coverage and are higher under RP than YP contracts. Revenue risk, measured by $\sqrt{Var^k_{jtm}}$, declines sharply with coverage.

Table 3. Insurance Characteristics

Statistic	Insurance	Corn	Soybeans	Wheat
$\mathbb{E}^k_{jtm}$	No Insurance	638	506	329
	(RP, 50%)	661	513	345
	(RP, 85%)	713	507	365
	(YP, 50%)	641	502	339
	(YP, 85%)	708	480	371
$\sqrt{Var}^k_{jtm}$	No Insurance	191	332	189
	(RP, 50%)	165	319	171
	(RP, 85%)	107	278	134
	(YP, 50%)	188	334	180
	(YP, 85%)	183	326	156

Notes: The table reports average insurance characteristics across crops and coverage levels for counties in Figure A1 between 2011 and 2019. Where available, I compare estimated and observed values. All measures are expressed in $ per acre.

Specification. The indirect utility in Equation (6) implies that the share of farmers in county m planting crop k who choose contract j in year t is given by the standard logit formula (Berry, 1994):

$$\sigma^k_{jmt} = \frac{\exp\left(\beta^E \Delta\mathbb{E}^k_{jtm} - \beta^V \Delta Var^k_{jtm} + \boldsymbol{\xi}^k_{jtm}\right)}{1 + \sum_{j' \neq 0} \exp\left(\beta^E \Delta\mathbb{E}^k_{j'tm} - \beta^V \Delta Var^k_{j'tm} + \boldsymbol{\xi}^k_{j'tm}\right)}. \tag{10}$$

I estimate the demand parameters by regressing log share ratios against relative mean and variance of net revenues:

$$\ln \frac{\sigma^k_{jmt}}{\sigma^k_{0mt}} = \beta^E \Delta\mathbb{E}^k_{jtm} - \beta^V \Delta Var^k_{jtm} + \boldsymbol{\xi}^k_{jmt}. \tag{11}$$

Identification. In the preferred specification identification comes from within-county-crop, year-to-year variation in the expected profits and risk exposure across insurance contracts. Local weather variability impacts the precision of yield beliefs, which determines the distance between each insurance product in the characteristics space: a spiked yield distribution shrinks the distance between insurance products, whereas a wide distribution increases it. Worldwide weather variability has a similar effect mediated through the spread of crop price distributions. Because the RMA ensures premiums are actuarially fair, they are exogenous to farmers' insurance demand (see Section 2).

Results. Table 4 shows that farmers place positive weight on higher expected revenues and dislike revenue risk. Across specifications, the coefficient on $\Delta\mathbb{E}$ is precisely estimated, while the coefficient on ΔVar is negative and significant in the preferred specification with county–commodity and year–

Table 4. Crop Insurance Demand

Dependent Variable:	$\ln \sigma^k_{jtm}/\sigma^k_{0tm}$		
	(1)	(2)	(3)
$\Delta\mathbb{E}^k_{jtm}$	3.086***	6.035***	6.866***
	(0.4558)	(0.4692)	(0.4546)
ΔVar^k_{jtm}	-18.86***	-41.25***	-43.39***
	(2.731)	(2.273)	(2.324)
County FE		Yes	
Year FE		Yes	
County-Crop FE			Yes
Year-Crop FE			Yes
Observations	370,396	370,396	370,396
R^2	0.012	0.195	0.240
Implied CARA (per 1,000$)	12.23	13.67	12.64
Implied RRA at outside option	4.503	5.035	4.655
Avg own premium elasticity	-0.070	-0.138	-0.157
Avg cross premium elasticity	0.095	0.185	0.211
Avg own risk elasticity	-1.097	-2.400	-2.524

Notes: The table presents the results from the estimation of crop insurance demand. $\Delta\mathbb{E}$ is expressed in thousand dollars per acre and ΔVar in million dollars per acre. The estimation sample includes all counties in Figure A1 between 2011 and 2019. Standard errors are clustered by state-year. Significance levels: *** p<0.01, ** p<0.05, * p<0.1.

commodity fixed effects. Mapping $(\hat{\beta}^E, \hat{\beta}^V)$ into the CARA utility function implies a coefficient of absolute risk aversion $\hat{\lambda} = 12$–14 per \$1,000, corresponding to a relative risk aversion of about 4.5–5.0 at the mean outside-option profit level.[23] The average own-premium elasticity is around -0.15, the cross-premium elasticity is about 0.20, and the average own risk elasticity with respect to revenue variance is approximately -2.5. The relatively low own-premium elasticity (in absolute value) is consistent with the fact that crop-insurance premiums are not competitively determined but administratively set, limiting the scope for price-based substitution across plans and dampening the responsiveness of enrollment to premium changes.

Table A9 in Appendix A3.2 shows that crop insurance demand is similar across county types. I split counties according to whether they have an above- or below-median share of large farms (Figure A10). In both groups, farmers value expected returns, with coefficients on $\Delta\mathbb{E}^k_{jtm}$ in the

[23] Empirical estimates of farmer relative risk aversion vary widely, ranging from values near 1 (Bar-Shira et al., 1997) to above 5 (Menapace et al., 2013), placing my estimates toward the higher end of this range.

Table 5. Effects of Removing Insurance Subsidies

	Δ Shares (percentage points)			Δ Exp. Static Profits ($/acre)
Commodity	Insured	RP | insured	Cov. ≥ 75 | insured	
Corn	-6.5	-3.1	-2.8	-52.7
Soybeans	-4.4	-1.0	-1.4	-35.2
Wheat	-4.6	-1.6	-1.5	-21.9

Notes: This table reports the effects of removing crop insurance premium subsidies on insurance take-up and expected producer surplus. Changes in insurance outcomes are expressed in percentage points. "Insured" denotes the share of acreage enrolled in any insured plan. "RP | insured" denotes the share of Revenue Protection contracts conditional on being insured, and "Cov. ≥ 75 | insured" denotes the share of insured acreage with coverage levels of at least 75 percent. Changes in expected static profits are reported in dollars per acre. All outcomes are averaged across counties within each commodity. Corn, soybean, and wheat acreage are held fixed at their average levels over 2011–2019. The sample includes all counties shown in Figure A1.

range of 6–7, and display negative and precisely estimated coefficients on ΔVar^k_{jtm}. A similar pattern emerges when counties are split by land quality (Figure A11).[24] Counties with above- and below-median shares of high-quality land exhibit comparable risk aversion. Overall, these results suggest that insurance demand reflects a similar trade-off between higher expected returns and reduced variance across counties with different farm structures and land endowments.

Finally, I conduct a static policy exercise in which premium subsidies are removed (Table 5). I recompute expected profits without subsidies, holding acreage and crop prices fixed, and predict insurance choices using the estimated demand system. Eliminating subsidies reduces insurance take-up across all three crops: relative to baseline coverage rates of about 80% for corn and soybeans and 60% for wheat, the insured share falls by roughly 4.5–6.5 percentage points (5–8 percent). Farmers who remain insured also adjust along the intensive margin, shifting toward contracts with lower coverage and less revenue protection, thereby reducing the degree of income risk protection provided by the program. Expected static profits decline by about $53 per acre for corn, $35 for soybeans, and $22 for wheat. These losses exceed the value of the foregone subsidies because crop insurance provides risk protection rather than a pure transfer: removing subsidies lowers coverage and therefore increases exposure to downside risk.

Because acreage and yield and price distributions are held fixed, these estimates capture only short-run, partial-equilibrium responses. The next section embeds the insurance demand system in the dynamic crop choice model to evaluate the full equilibrium effects of subsidy design.

[24]The land quality index is a function of time-invariant characteristics such as soil type, elevation, and ruggedness (Soil Survey Staff, 2024). I select the median quality threshold and aggregate this index into two levels.

5.2 Crop Choice

I estimate the dynamic crop-choice model by maximum likelihood using a nested fixed point algorithm (Rust, 1987). Unlike the static insurance-demand block, the dynamic problem must be solved over the full state space, including aggregate acreage states that are not directly observed in the data. In addition, climate change makes the environment non-stationary, so expected yields and revenue risk evolve over time as weather distributions shift. I therefore construct payoff objects for all aggregate acreage states and for future years through 2050.

Yield and price beliefs and payoff inputs. Constructing the expected net static profits $\mathbb{E}^*_{kmt}(s)$, which feed into dynamic payoffs, requires beliefs about yields and prices at planting time.

I assume farmers have accurate beliefs about future climate conditions, approximated by the projections from six climate models (see Section 3.1) under a moderate emissions scenario. In other words, farmers do not know future realization of weather, but they know how weather distributions shift over time. As in Section 5.1, I combine pre-planting weather data with weather–yield relationship to construct planting-time beliefs about the distribution of local yields for each county m, crop k, and year t.

Because prices depend on aggregate production, farmers must also form beliefs about national acreage and global yields. I discretize the aggregate acreage component of the state space. Let $s_t \in \{1, \ldots, S\}$ denote a discrete aggregate acreage state that bins the national planted-acreage vector across the four land uses. Farmers are assumed to have rational expectations about the evolution of this state, described by the perceived law of motion $\Pi(s'|s)$ estimated from national acreage data. In addition, farmers have accurate beliefs about future national yields in the U.S. and the rest of the world based on the climate projections. I combine these yield projections with the inverse-demand system described in Appendix A2 to construct planting-time price beliefs conditional on (t, s).

Given these yield and price beliefs, I compute revenues, actuarially fair premiums, and expected indemnities for each insurance contract. Combining these objects with the estimated insurance demand system yields the planting-time expected net static profits under the optimal insurance choice, $\mathbb{E}^*_{kmt}(s)$, for each crop k, county m, calendar year t, and aggregate state s (see Appendix A4.1).

Estimation by nested fixed point maximum likelihood. Let $\Theta = \{\alpha, \{\phi_{k'',k'\to k}\}_{k'',k',k}\}$ denote the dynamic crop-choice parameter vector introduced in Section 4.2.3.

Inner loop. For a candidate Θ, I solve the farmer's dynamic discrete choice problem on the discretized state space $\{k'', k', m, t, s\}$, taking as given the payoff inputs $\mathbb{E}^*_{kmt}(s)$ and the perceived law of motion for aggregate acreage $\Pi(s'|s)$. The solution yields model-implied CCPs, which take the multinomial logit form under the i.i.d. type-I extreme value assumption on idiosyncratic shocks. Because climate change makes the environment non-stationary, I solve a finite-horizon problem by backward recursion over calendar time. The terminal year is set to 2050, after which I impose a stationary continuation value. Appendix A4.2 provides details.

Outer loop. Using land-use transitions constructed from the CDL, I form county-level transition counts $N_{k'',k'\to k,mt}$. For each candidate Θ, I evaluate the multinomial log-likelihood implied by the inner-loop CCPs and choose Θ to maximize

$$\ell(\Theta) = \sum_{m,t,k'',k'} \sum_{k} N_{k'',k'\to k,mt} \log P_{k'',k'\to k,mt}(\Theta). \tag{12}$$

Identification and normalizations. Because utilities are only identified up to location and scale in logit models, I impose standard normalizations. I take fallow as the outside option and set $\phi_{k'',k'\to f} \equiv 0$ for all histories $\{(k'', k')\}$, and $\mathbb{E}^*_{fmt}(s) \equiv 0$. Finally, I normalize the scale of the i.i.d. type-I extreme value shocks.

Under these normalizations, the profit sensitivity parameter α is identified from within-county changes over time in relative expected net returns $\mathbb{E}^*_{kmt}(s)$ across crops, driven by plausibly exogenous variation in (i) local yield risk and expected yields, (ii) global yield realizations, and (iii) aggregate market conditions summarized by s that shift equilibrium prices through the demand-and-trade block. The history-dependent terms $\phi_{k'',k'\to k}$ are identified from systematic differences in persistence and switching patterns across rotation histories, conditional on expected net returns.

Results. Table 6 reports the estimated parameters governing dynamic crop choice. Panel A reports $\hat{\alpha}$, the coefficient that scales expected net static profits in the per-period payoff function (Equation 8). Panel B reports the history-dependent term $\phi_{k'',k'\to k}$, which depends on the crops planted in the previous two years and is normalized to have mean zero within each destination crop k. The estimates show substantial heterogeneity across histories—often on the order of several hun-

Table 6. Dynamic Crop Choice Estimates

Panel A. Flow profits			
α	0.0010		
	(0.0002)		
Panel B. Path-dependent term ϕ ($/acre)			
	Corn	Soybeans	Wheat
Corn-Corn	2326	1550	695
	(499)	(364)	(100)
Soybeans-Corn	998	2674	-687
	(128)	(570)	(326)
Wheat-Corn	-702	-187	786
	(189)	(113)	(184)
Fallow-Corn	-1563	-1218	-1889
	(174)	(71)	(387)
Corn-Soybeans	2761	1696	889
	(560)	(322)	(103)
Soybeans-Soybeans	1149	2511	965
	(180)	(499)	(127)
Wheat-Soybeans	-127	1349	2042
	(70)	(332)	(514)
Fallow-Soybeans	-1683	-752	-2161
	(118)	(75)	(334)
Corn-Wheat	2124	-161	1119
	(486)	(118)	(248)
Soybeans-Wheat	2316	2434	1030
	(450)	(482)	(169)
Wheat-Wheat	629	-316	2218
	(128)	(122)	(620)
Fallow-Wheat	-532	-3159	-707
	(107)	(685)	(126)
Corn-Fallow	420	-203	779
	(70)	(53)	(211)
Soybeans-Fallow	-770	743	-1798
	(147)	(137)	(293)
Wheat-Fallow	-2144	-2239	1326
	(583)	(595)	(290)
Fallow-Fallow	-5201	-4720	-4608
	(1210)	(1144)	(1018)

Notes: Panel A reports the estimated coefficient α that scales expected net static profits in the per-period payoff function (see Equation (8)). Panel B reports the state-dependent term ϕ in dollars per acre. The path-dependent terms are normalized to have mean zero within each destination crop, so the reported coefficients reflect relative switching costs across previous crop states. The crop-specific intercepts range between -2,595 and -2,420 dollars per acre. Bootstrap standard errors are reported in parentheses.

dred dollars per acre—consistent with economically important rotation-related complementarities and adjustment frictions. Together, α and ϕ generate persistence in land use and discipline the model's transition patterns across crops in the counterfactual simulations.

To gauge the responsiveness of planting decisions to insurance incentives, I compute long-run acreage elasticities with respect to premium-subsidy exposure by simulating permanent changes in subsidy schedules. A 10% proportional increase in subsidy exposure across all crops raises total cultivated acreage by about 0.12%. Crop-specific elasticities range from 0.009 for corn to 0.015 for soybeans and wheat, with cross-crop responses roughly an order of magnitude smaller. Although smaller than the county-crop elasticities reported by Yu et al. (2018), these estimates imply economically meaningful responses once scaled by the share of subsidies in expected returns (see Appendix A4.3 for details).

Appendix A4.3 also reports additional robustness and model-fit diagnostics. Re-estimating the model using only years prior to 2018—before changes in the CDL classification procedure that may mechanically increase persistence—yields parameter estimates very similar to the baseline. Finally, comparing model-implied conditional choice probabilities (CCPs) to those measured in the data shows that the model reproduces the main cross-sectional planting decisions across counties and rotation histories.

6 Crop Insurance Subsidies in a Changing Climate

In this section, I evaluate how alternative crop insurance subsidy designs reallocate protection across farmers while shaping long-run adaptation to climate change. I simulate equilibrium paths of land use, insurance choices, and crop prices under alternative subsidy regimes between 2020 and 2050.[25]

Throughout this section, I summarize policy outcomes using farmer surplus and insured exposure. Farmer surplus measures the program's intended benefit to producers and is the sum of value

[25] I assume the U.S. Department of Agriculture commits to a path of crop insurance subsidies over 2020–2050 and that government policies in the rest of the world are fixed. Counties outside the selected sample (Figure A1) receive status quo subsidies (Table A1) in all counterfactual scenarios. As for the dynamic estimation, each counterfactual combines projected climate paths with the reduced-form inverse-demand system to update planting-time beliefs about yields, prices, premiums, and expected net returns, $\mathbb{E}^*_{kmt}(s_t)$; see Appendix A4 for details. For a given perceived law of motion of aggregate acreage, I solve farmers' optimal planting and insurance decisions using the same dynamic programming structure as in the estimation. These decisions imply a new aggregate acreage path, which in turn updates planting-time beliefs. An equilibrium is a fixed point in which the perceived law of motion used to form expectations coincides with the law of motion generated by optimal behavior under the policy.

functions across counties and two-year land use choices. Insured exposure measures the amount of production whose downside risk is effectively backed by the program, defined as insured acreage weighted by expected indemnities. It is the natural counterpart to farmer surplus in this setting because it captures not only how much insurance is purchased, but also whether subsidies reallocate production toward riskier crops and locations. These two objects therefore provide a transparent summary of the main policy trade-off in the paper: protection versus adaptation.

I begin by quantifying the effects of the status quo subsidy relative to a no-subsidy benchmark. I then ask whether a simple forward-looking targeting rule—one that varies subsidy generosity with projected regional climate-risk trends—can improve on the status quo. I refer to this set of policies as *By Region*. Finally, I consider transfers that are decoupled from actuarial risk but remain conditional on insurance take-up. I refer to this set of policies as *Unconditional*.

6.1 Impact of Status Quo Subsidies

Table 7 shows that the status quo subsidy schedule does provide protection to farmers.[26] Relative to the no-subsidy benchmark, farmer surplus rises by 1.02%, the insured share of cultivated acreage rises by 2.13 percentage points, and insured farmers choose slightly more generous contracts: the share enrolled in Revenue Protection rises by 0.75 percentage points and the share with coverage of at least 75% rises by 1.08 percentage points.[27]

At the same time, the program is a blunt way to transfer resources to farmers. Government spending is $2.34 billion annually, while farmer surplus rises by only $0.92 per $100 of public spending. Several channels dissipate the transfer. First, subsidies expand cultivated acreage by 1.72% and increase production of all three crops, which puts downward pressure on crop prices and reduces farm revenues in equilibrium. Second, part of the subsidy finances additional insurance coverage and more generous contracts, which increase risk protection but do not translate one-for-one into higher profits.

The policy also increases the government's exposure to agricultural risk by 5.72%. Part of this increase is mechanical and potentially desirable from the Department of Agriculture's perspective:

[26] All counterfactual outcomes are averaged over 2030–2050. I exclude the first decade of the simulation because it is more sensitive to initial conditions. Averaging over 2030–2050 instead highlights implications of subsidy design once the system has begun to adjust, while also smoothing transitory year-to-year fluctuations in weather.

[27] These changes in insurance participation are smaller than in the static counterfactual reported in Table 5. In the static exercise, acreage and crop prices are held fixed, so the effect of subsidies operates only through insurance demand. In contrast, in the dynamic equilibrium, land use and price adjustments partially offsets the incentives to adjust insurance coverage.

Table 7. Counterfactual Results

Scenario:	No subsidies (1)	Status quo (2)	By region (3)	Unconditional (4)
Panel A. Aggregate outcomes				
Government spending	0.00	2,336.04	2,248.89	1,694.70
Farmer surplus	2,121.02	1.02%	1.06%	1.00%
Farmer surplus per $100 of spending		0.92	1.00	1.25
Insured exposure	21.44	5.72%	4.40%	3.34%
Panel B. Agricultural outcomes				
Cultivated acres	133.83	1.72%	1.55%	1.60%
Corn acres	58.23	0.99%	0.60%	1.43%
Corn prices	137.28	-1.24%	-0.55%	-0.27%
Corn production	227.84	0.83%	0.51%	1.30%
Soy acres	59.10	2.42%	2.24%	1.70%
Soy prices	271.49	-0.26%	-0.03%	0.01%
Soy production	78.40	2.36%	2.22%	1.65%
Wheat acres	16.49	1.79%	2.44%	1.88%
Wheat prices	161.06	-0.27%	-0.23%	-0.34%
Wheat production	23.66	1.48%	1.98%	1.53%
Panel C. Insurance participation				
Share insured	81.37%	2.13 p.p.	1.48 p.p.	1.77 p.p.
Share insured in RP | insured	89.18%	0.75 p.p.	0.68 p.p.	-0.15 p.p.
Share insured, Cov. >= 75% | insured	68.04%	1.08 p.p.	0.99 p.p.	-0.15 p.p.

Notes: The table reports simulated counterfactual outcomes over the period 2030–2050. Column (1) reports average levels under the "No subsidies" counterfactual. Columns (2)–(4) report the effects of alternative policy scenarios relative to the "No subsidies" counterfactual. In the "Status Quo" scenario, subsidies are proportional to premiums. In the "By Region" scenario, subsidies remain proportional to premiums, but their generosity varies with the local trend in climate risk (-100% (+50%) in region with steep (shallow) increases in the variability of extreme degree days; see Figure A18). In the "Unconditional" scenario, subsidies take the form of lump-sum payments conditional on purchasing insurance and do not depend on actuarial risk (15$ per insured acre). In Panel A, government spending is measured in millions of dollars. Farmer surplus is similarly expressed in millions of dollars and is the aggregation of the value function (Equation (9)) aggregated across counties and land use. Insured exposure is reported in acre-equivalent units. In Panel B, acreage and production variables are reported in millions of acres and millions of tons, respectively. Prices are expressed in dollars per ton. Panel C reports insurance participation outcomes: the insured share of cultivated acreage, the share of insured acreage with coverage $\geq$ 75%, and the share of insured acreage enrolled in Revenue Protection (RP).

subsidies induce greater insurance participation and somewhat more generous coverage. But Table 7 also shows that the program expands cultivated acreage, implying that exposure rises not only because more existing production is insured, but also because more land is brought into production.

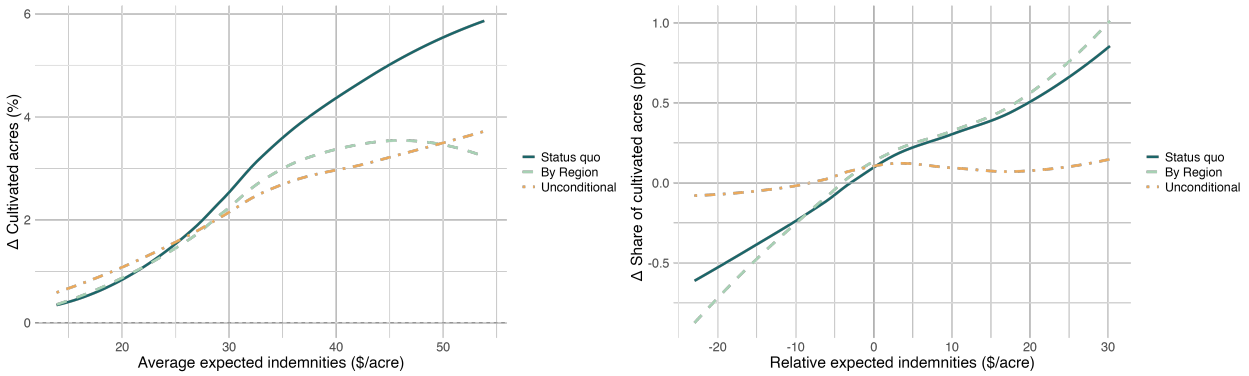
Figure 5 shows that this additional exposure is not evenly distributed. Across counties (Panel A), the status quo expands cultivation disproportionately in counties with higher expected indemnities. In a county where average expected indemnities are about $40 per acre, the status quo subsidy schedule increases cultivated acreage by roughly 3.5% relative to the no-subsidy benchmark. By contrast, counties with much lower actuarial risk experience substantially smaller acreage responses. Within counties (Panel B), it shifts crop shares toward crops with above-average expected indemnities. Thus, the increase in insured exposure reflects four channels: more insurance participation, more cultivated land, more cultivation in riskier locations, and more acreage in riskier crops. The last two margins are the key sense in which premium-linked subsidies distort adaptation incentives.

Consistent with these patterns, Appendix Figure A20 shows that the acreage response under the status quo is concentrated in crops and locations most exposed to extreme heat. Corn and soybean acreage increases are largest in the southern half of the sample, where projected increases in extreme degree days are strongest and where these crops are most sensitive to heat exposure (see Figures 1 and 2). By contrast, changes in wheat acreage are more spatially dispersed. This reflects the weaker relationship between wheat yields and extreme heat documented in Table 2 and the more heterogeneous regional impacts of climate change on wheat productivity.

Appendix Figure A21 shows that these distortions intensify over time as climate change unfolds. Panel A compares the evolution of cultivated acreage in counties at the bottom and top deciles of the expected-indemnity distribution. Under the status quo, acreage expansion becomes increasingly concentrated in the riskiest counties: by 2050, cultivated acreage rises by nearly 8% in counties in the top decile of expected indemnities, compared with less than 1% in the safest counties. Panel B shows a similar pattern within counties: crops with above-average expected indemnities steadily gain acreage share over time, while safer crops lose share. In the model, this amplification is reinforced by adjustment frictions: because switching crops is costly, farmers adapt only gradually to evolving climate conditions. Status quo subsidies therefore not only distort planting decisions at a point in time but also slow the reallocation of land toward more resilient crops and locations.

Overall, the status quo buys protection by subsidizing risk itself: it raises surplus today, but it also weakens the reallocation of land away from increasingly vulnerable locations and crops.

Figure 5. Crop Insurance Subsidies Induced Land Use Distortions



(A) Across counties **(B)** Within county

Notes: The figure illustrates how crop insurance premium subsidies distort land-use decisions under alternative subsidy schedules over the period 2030–2050. In the "Status Quo" scenario, subsidies are proportional to actuarially fair premiums. In the "By Region" scenario, subsidies remain proportional to premiums but their generosity varies with the local trend in climate risk. In the "Unconditional" scenario, subsidies take the form of lump-sum payments conditional on purchasing insurance and do not depend on actuarial risk. Panel (A) shows distortions across counties. The horizontal axis reports the county-level average of expected indemnities, which summarizes local production risk. The vertical axis reports the percentage change in cultivated acreage relative to the no-subsidy counterfactual. Panel (B) shows distortions within counties across crops. The horizontal axis reports crop-specific expected indemnities relative to the county-year average, capturing how risky a crop is relative to other crops available locally. The vertical axis reports the change in the crop's share of cultivated acreage (in percentage points) relative to the no-subsidy counterfactual. Lines are best-fit curves weighted by baseline acreage in the no-subsidy equilibrium.

6.2 Targeting Subsidies by Future Climate-risk Trends

One question is whether a simple forward-looking targeting of subsidies can preserve the short-run protection provided by crop insurance while reducing the tendency of the status quo to keep land in increasingly vulnerable places. I therefore consider a low-dimensional *By Region* policy that retains the premium-based structure of the program but allows subsidy generosity to vary with projected regional climate risk trends. Counties are grouped according to whether the projected trend in the variability of extreme degree days is *steep* or *shallow* (Figure A18). Appendix Figure A19 panel A summarizes the resulting policy frontier. Among this set of policies, I focus on the reform that minimizes aggregate insured exposure subject to farmer surplus equal to the status quo.[28] In the selected reform, subsidies are eliminated in counties facing steep increases in climate risk and increased by 50% in counties where risk trends are flatter.

This policy improves on the status quo along several dimensions. By design, relative to the status quo, farmer surplus remains essentially unchanged while insured exposure falls from 5.72% to 4.40%. Government spending also declines, from $2.34 billion to $2.25 billion, so farmer surplus per $100

[28] Appendix Figure A19 panel A suggests there exist policies delivering smaller decreases in insured exposure than the selected *By Region* policy while increasing farmer surplus on average.

of public spending rises from 0.92 to 1.00.

The reduction in insured exposure reflects two forces. Part of the effect reflects the smaller expansion of insurance participation relative to the status quo (-0.65 percentage points) and cultivated acreage (-0.2 percentage points, or about 270 thousand acres). But the reform also changes where production takes place. In particular, the targeting rule reallocates support away from counties where climate risk is projected to worsen most rapidly.

Figure 5 panel A illustrates this mechanism. The positive relationship between risk and acreage expansion becomes noticeably flatter under *By Region*. Counties with high expected indemnities—which tend to also face the largest projected increases in climate risk—no longer receive the same subsidy support as counties where climate risk evolves more favorably. In that sense, the reform encourages adaptation by allowing cultivated land to reallocate in response to climate-risk trends rather than continuing to reward risk-taking production everywhere. This improvement is driven primarily by a reduction in acreage expansion in the most exposed counties (Appendix Figure A21).

The composition of acreage changes reflects this spatial reallocation. Relative to the status quo, the *By Region* policy sharply attenuates corn expansion, with corn acreage rising by only 0.60% instead of 0.99%. Soybean expansion also declines slightly, from 2.42% to 2.24%. By contrast, wheat acreage rises more under *By Region* than under the status quo, 2.44% versus 1.79%. This pattern is consistent with the climate sensitivities documented in Section 3: as support is reallocated away from regions where extreme heat risk is worsening most rapidly, land shifts away from the crops most prevalent in those regions.[29]

Despite these improvements, region targeting leaves an important distortion intact. Figure 5 panel B shows that within counties, crops with higher expected indemnities continue to gain acreage relative to lower-indemnity crops. In other words, the relationship between crop-level risk and acreage expansion within a county remains largely unchanged under *By Region*. This reflects the fact that subsidies remain proportional to premiums, so the policy continues to reward crops with higher actuarial risk within a county-year. The main gains from *By Region* come from correcting the spatial allocation of cultivation across counties, while the within-county tilt toward higher-risk crops remains largely intact.

[29] Appendix Figure A20 confirms this intuition. Relative to the status quo, corn expansion is especially reduced in the southern half of the sample, where projected increases in extreme degree days are strongest. Wheat gains are more pronounced in the northern half of the sample, in regions where climate risk evolves less adversely.

6.3 Decoupling subsidies from risk

An alternative approach is to remove the link between subsidies and actuarial risk altogether. I therefore consider a set of *Unconditional* policies in which farmers receive a per-acre transfer conditional on purchasing insurance but independent of expected indemnities. These transfers resemble the direct payments that were phased out in the 2014 Farm Bill in that they provide income support without rewarding risk-taking behavior, although the historical program was fully decoupled from production and insurance decisions. Appendix Figure A19 panel B summarizes the policy frontier generated by varying the level of the unconditional payment. As in the previous subsection, I focus on the policy that minimizes aggregate insured exposure subject to farmer surplus equal to the status quo.

Table 7 shows that decoupling support from actuarial risk leads to a further reduction in insured exposure relative to the *By Region* reform. Government spending also declines, implying that farmer surplus per $100 of public spending increases relative to both the status quo and the targeted policy. The reform still expands insurance participation and cultivated acreage relative to the no-subsidy benchmark, but these responses are smaller than under the premium-linked subsidy schedule.

Importantly, insurance participation no longer tilts toward the most generous contracts: the share of insured acreage enrolled in Revenue Protection and the share with coverage above 75% both decline slightly relative to the no-subsidy benchmark (-0.15 percentage points). This pattern reflects the removal of the premium-risk linkage. Under the status quo, although subsidy rates decline with coverage (Appendix Table A1), premiums increase sharply with expected indemnities, so contracts with higher coverage and Revenue Protection still receive larger subsidy dollars. Once transfers are decoupled from premiums, insurance participation expands without disproportionately subsidizing high-coverage or Revenue Protection contracts.

A key difference relative to the *By Region* reform is that unconditional transfers eliminate the incentive to reallocate acreage toward riskier crops within a county. Figure 5 shows that while region targeting mainly attenuates the across-county distortion (Panel A), unconditional transfers flatten both relationships.[30] In Panel B, the link between crop-specific relative risk and acreage changes essentially disappears: because payments are no longer tied to actuarial risk, crops with

[30]Some across-county distortion nevertheless remains under the *Unconditional* policy. Decoupling transfers from actuarial risk does not eliminate the subsidy to insured production itself. Counties where insurance is more valuable therefore still expand relative to the no-subsidy benchmark.

higher expected indemnities do not receive larger subsidy dollars. In this sense, unconditional transfers remove both margins of insurance-induced distortion while preserving the income-support role of the program.

Taken together, these results suggest that the main source of distortion in the crop insurance program arises from tying subsidies to actuarial risk rather than from subsidizing insurance participation per se. Decoupling transfers from expected indemnities preserves much of the short-run protection value of the program while largely removing the incentives that shift production toward riskier crops and locations.

7 Conclusion

This paper develops a dynamic framework to study how crop insurance subsidies shape agricultural adaptation to climate change. I show that the current U.S. subsidy schedule provides short-run protection to farmers but weakens adaptation incentives. Because subsidies are tied to actuarial risk, they encourage production in riskier crops and locations and increase insured exposure—the amount of agricultural output whose downside risk is effectively backed by the program.

A simple forward-looking reform that varies subsidy generosity with projected regional climate trends improves on the status quo by reallocating support away from areas where climate risk is expected to worsen. However, the largest reduction in insurance-induced distortions arises when transfers are decoupled from actuarial risk altogether. These results highlight that the design of climate-risk insurance programs plays a central role in shaping long-run adaptation to climate change.

The analysis focuses on one margin of adaptation—crop switching—because this is the dimension for which consistent field-level data are available over long time horizons. In practice, farmers may also adapt along other margins, including crop variety adoption, irrigation investment, or changes in input use. The framework developed here is sufficiently general to incorporate these choices as additional decision margins. In particular, it could be used to study whether crop insurance subsidies discourage the adoption of climate-resilient seed varieties or other risk-reducing technologies. Extending the analysis to these margins is a promising direction for future research.

References

Al-Kaisi, M. M., S. V. Archontoulis, D. Kwaw-Mensah, and F. Miguez (2015): "Tillage and crop rotation effects on corn agronomic response and economic return at seven Iowa locations," *Agronomy Journal*, 107, 1411–1424.

Allan, R. P., P. A. Arias, S. Berger, J. G. Canadell, C. Cassou, D. Chen, A. Cherchi, S. L. Connors, E. Coppola, F. A. Cruz, et al. (2023): "Intergovernmental Panel on Climate Change (IPCC). Summary for Policymakers," in *Climate change 2021: The physical science basis. Contribution of working group I to the sixth assessment report of the intergovernmental panel on climate change*, Cambridge University Press, 3–32.

Allcott, H., C. Knittel, and D. Taubinsky (2015): "Tagging and targeting of energy efficiency subsidies," *American Economic Review*, 105, 187–191.

Annan, F. and W. Schlenker (2015): "Federal crop insurance and the disincentive to adapt to extreme heat," *American Economic Review*, 105, 262–266.

Araujo, R., F. Costa, and M. SantAnna (2026): "Efficient conservation of the Brazilian Amazon: Estimates from a dynamic model," *Review of Economic Studies*, 93, 72–105.

Bakhsh, A. and R. S. Kanwar (2007): "Tillage and N application rates affect on corn and soybean yields and NO3-N leaching losses," *Transactions of the ASABE*, 50, 1189–1198.

Bar-Shira, Z., R. E. Just, and D. Zilberman (1997): "Estimation of farmers' risk attitude: an econometric approach," *Agricultural Economics*, 17, 211–222.

Baylis, P. and J. Boomhower (2023): "The economic incidence of wildfire suppression in the United States," *American Economic Journal: Applied Economics*, 15, 442–473.

Baylis, P. W. and J. Boomhower (2026): "Mandated versus Voluntary Adaptation to Natural Disasters: The Case of US Wildfires," *Journal of Political Economy*.

Berry, S. T. (1994): "Estimating discrete-choice models of product differentiation," *The RAND Journal of Economics*, 242–262.

Boryan, C., Z. Yang, R. Mueller, and M. Craig (2011): "Monitoring US agriculture: the US department of agriculture, national agricultural statistics service, cropland data layer program," *Geocarto International*, 26, 341–358.

Bulut, H., K. J. Collins, and T. P. Zacharias (2012): "Optimal Coverage Level Choice with Individual and Area Insurance Plans," *American Journal of Agricultural Economics*, 94, 1246–1252.

Burke, M. and K. Emerick (2016): "Adaptation to climate change: Evidence from US agriculture," *American Economic Journal: Economic Policy*, 8, 106–140.

Burlig, F., A. Jina, E. M. Kelley, G. V. Lane, and H. Sahai (2025): "The value of forecasts: Experimental evidence from India," Tech. rep., National Bureau of Economic Research.

Burlig, F., L. Preonas, and M. Woerman (2026): "Groundwater and Crop Choice in the Short and Long Run," Tech. rep., National Bureau of Economic Research.

Claassen, R., C. Langpap, and J. Wu (2017): "Impacts of federal crop insurance on land use and environmental quality," *American Journal of Agricultural Economics*, 99, 592–613.

Coble, K. H., T. O. Knight, R. D. Pope, and J. R. Williams (1996): "Modeling farm-level crop insurance demand with panel data," *American Journal of Agricultural Economics*, 78, 439–447.

Congressional Research Service (2021): "Federal Crop Insurance: A Primer," Accessed: 25 September 2024.

Cornaggia, J. (2013): "Does risk management matter? Evidence from the US agricultural industry," *Journal of Financial Economics*, 109, 419–440.

Costinot, A., D. Donaldson, and C. Smith (2016): "Evolving comparative advantage and the impact of climate change in agricultural markets: Evidence from 1.7 million fields around the world," *Journal of Political Economy*, 124, 205–248.

Cui, X. (2020): "Climate Change and Adaptation in Agriculture: Evidence from US Cropping Patterns," *Journal of Environmental Economics and Management*, 101, 102306.

Deryugina, T. and M. Konar (2017): "Impacts of crop insurance on water withdrawals for irrigation," *Advances in Water Resources*, 110, 437–444.

Diffenbaugh, N. S., F. V. Davenport, and M. Burke (2021): "Historical warming has increased US crop insurance losses," *Environmental Research Letters*, 16, 084025.

Dominguez-Iino, T. (2026): "Efficiency and redistribution in environmental policy: An equilibrium analysis of agricultural supply chains," *Journal of Political Economy*.

Druckenmiller, H., Y. Liao, S. Pesek, M. Walls, and S. Zhang (2024): "Removing development incentives in risky areas promotes climate adaptation," *Nature Climate Change*, 14, 936–942.

Duflo, E., M. Greenstone, R. Pande, and N. Ryan (2018): "The value of regulatory discretion: Estimates from environmental inspections in India," *Econometrica*, 86, 2123–2160.

Ferreira, S. (2024): "Extreme weather events and climate change: Economic impacts and adaptation policies," *Annual Review of Resource Economics*, 16, 207–231.

Fried, S. (2022): "Seawalls and stilts: A quantitative macro study of climate adaptation," *The Review of Economic Studies*, 89, 3303–3344.

Gammans, M., P. Mérel, and A. Ortiz-Bobea (2017): "Negative impacts of climate change on cereal yields: statistical evidence from France," *Environmental Research Letters*, 12, 054007.

Gerarden, T. D. and M. Yang (2023): "Using targeting to optimize program design: evidence from an energy conservation experiment," *Journal of the Association of Environmental and Resource Economists*, 10, 687–716.

Glauber, J. W. (2013): "The growth of the federal crop insurance program, 19902011," *American Journal of Agricultural Economics*, 95, 482–488.

Goodwin, B. K. (1993): "An empirical analysis of the demand for multiple peril crop insurance," *American journal of agricultural economics*, 75, 425–434.

Goodwin, B. K., M. L. Vandeveer, and J. L. Deal (2004): "An empirical analysis of acreage effects of participation in the federal crop insurance program," *American Journal of Agricultural Economics*, 86, 1058–1077.

Hsiao, A. (2025): "Sea Level Rise and Urban Adaptation in Jakarta," Working paper.

Hultgren, A., T. Carleton, M. Delgado, D. R. Gergel, M. Greenstone, T. Houser, S. Hsiang, A. Jina, R. E. Kopp, S. B. Malevich, et al. (2025): "Impacts of climate change on global agriculture accounting for adaptation," *Nature*, 642, 644–652.

IPCC (2022): "Summary for Policymakers," in *Climate Change 2022: Impacts, Adaptation and Vulnerability. Contribution of Working Group II to the Sixth Assessment Report of the Intergovernmental Panel on Climate Change*, ed. by H.-O. Pörtner, D. Roberts, E. Poloczanska, K. Mintenbeck, A. Alegría, M. Craig, S. Langsdorf, S. Löschke, V. Möller, A. Okem, and B. Rama, Cambridge, UK and New York, NY, USA: Cambridge University Press.

Jones, B., J. Moscona, B. A. Olken, and C. von Dessauer (2026): "With or Without U? Binning Bias and the Causal Effects of Temperature Extremes," Tech. rep., National Bureau of Economic Research.

Karlan, D., R. Osei, I. Osei-Akoto, and C. Udry (2014): "Agricultural decisions after relaxing credit and risk constraints," *The Quarterly Journal of Economics*, 129, 597–652.

Kirwan, B. E. (2009): "The incidence of US agricultural subsidies on farmland rental rates," *Journal of political economy*, 117, 138–164.

Kousky, C. (2019): "The role of natural disaster insurance in recovery and risk reduction," *Annual Review of Resource Economics*, 11, 399–418.

Kousky, C., H. Kunreuther, S. Xian, and N. Lin (2021): "Adapting our flood risk policies to changing conditions," *Risk analysis*, 41, 1739–1743.

Krusell, P. and A. A. Smith, Jr (1998): "Income and wealth heterogeneity in the macroeconomy," *Journal of political Economy*, 106, 867–896.

MacDonald, J. M. (2020): "Corn and Soybean Farmers Combine Futures, Options, and Marketing Contracts To Manage Financial Risks," Accessed: 11 October 2024.

Mach, K. J., C. M. Kraan, M. Hino, A. Siders, E. M. Johnston, and C. B. Field (2019): "Managed retreat through voluntary buyouts of flood-prone properties," *Science Advances*.

McFadden, J., D. Smith, S. Wechsler, and S. Wallander (2019): "Development, adoption, and management of drought-tolerant corn in the United States," Tech. rep., US Department of Agriculture, Economic Research Service.

Menapace, L., G. Colson, and R. Raffaelli (2013): "Risk aversion, subjective beliefs, and farmer risk management strategies," *American Journal of Agricultural Economics*, 95, 384–389.

Mieno, T., C. G. Walters, and L. E. Fulginiti (2018): "Input use under crop insurance: the role of actual production history," *American Journal of Agricultural Economics*, 100, 1469–1485.

Moscona, J. and K. Sastry (2025): "Inappropriate technology: Evidence from global agriculture," Tech. rep., National Bureau of Economic Research.

Nelson, C. H. and E. T. Loehman (1987): "Further toward a theory of agricultural insurance," *American Journal of Agricultural Economics*, 69, 523–531.

O'Donoghue, E. (2014): "The effects of premium subsidies on demand for crop insurance," *USDA-ERS economic research report*.

OECD (2021): *Enhancing Financial Protection Against Catastrophe Risks*, OECD Publishing.

Peng, Y., L. Wang, P.-A. Jacinthe, and W. Ren (2024): "Global synthesis of cover crop impacts on main crop yield," *Field Crops Research*, 310.

PRISM Climate Group (2014): "Gridded Climate Data," Oregon State University.

Ramirez, O. A. and J. S. Shonkwiler (2017): "A probabilistic model of the crop insurance purchase decision," *Journal of Agricultural and Resource Economics*, 10–26.

Richards, T. J. (2000): "A two-stage model of the demand for specialty crop insurance," *Journal of agricultural and resource economics*, 177–194.

Rising, J. and N. Devineni (2020): "Crop switching reduces agricultural losses from climate change in the United States by half under RCP 8.5," *Nature communications*, 11, 4991.

RMA, U. R. M. A. (2023a): "Actuarial Information Browser," Accessed: 10 May 2023.

——— (2023b): "Summary of Business," Accessed: 10 May 2023.

Ruis, S., S. Stepanovic, and H. Blanco-Canqui (2023): "Intensifying a crop–fallow system: impacts on soil properties, crop yields, and economics," *Renewable Agriculture and Food Systems*, 38.

Russo, A. and K. Aspelund (2024): "Additionality and Asymmetric Information in Environmental Markets: Evidence from Conservation Auctions," Working paper.

Rust, J. (1987): "Optimal replacement of GMC bus engines: An empirical model of Harold Zurcher," *Econometrica: Journal of the Econometric Society*, 999–1033.

Schlenker, W., W. M. Hanemann, and A. C. Fisher (2006): "The impact of global warming on US agriculture: an econometric analysis of optimal growing conditions," *Review of Economics and statistics*, 88, 113–125.

Schlenker, W. and M. J. Roberts (2009): "Nonlinear temperature effects indicate severe damages to US crop yields under climate change," *Proceedings of the National Academy of sciences*, 106, 15594–15598.

Scott, P. (2014): "Dynamic discrete choice estimation of agricultural land use," Working Paper.

Sindelar, A. J., M. R. Schmer, V. L. Jin, B. J. Wienhold, and G. E. Varvel (2015): "Long-term corn and soybean response to crop rotation and tillage," *Agronomy Journal*, 107, 2241–2252.

Smith, V. H. and B. K. Goodwin (1996): "Crop insurance, moral hazard, and agricultural chemical use," *American Journal of Agricultural Economics*, 78, 428–438.

Soil Survey Staff, Natural Resources Conservation Service, U. S. D. o. A. (2024): "Web Soil Survey," Accessed 10 February 2024.

Suchato, P., T. Mieno, K. Schoengold, and T. Foster (2022): "The potential for moral hazard behavior in irrigation decisions under crop insurance," *Agricultural Economics*, 53, 257–273.

Thrasher, B., W. Wang, A. Michaelis, F. Melton, T. Lee, and R. Nemani (2022): "NASA global daily downscaled projections, CMIP6," *Scientific data*, 9, 262.

Tsiboe, F. and D. Turner (2023): "The crop insurance demand response to premium subsidies: Evidence from US agriculture," *Food Policy*, 119, 102505.

Wagner, K. R. (2022): "Adaptation and adverse selection in markets for natural disaster insurance," *American Economic Journal: Economic Policy*, 14, 380–421.

Wallander, S. (2013): "While Crop Rotations Are Common, Cover Crops Remain Rare," Accessed: 2 October 2024.

Walters, C. G., C. R. Shumway, H. H. Chouinard, and P. R. Wandschneider (2012): "Crop insurance, land allocation, and the environment," *Journal of Agricultural and Resource Economics*, 301–320.

Wang, R., R. M. Rejesus, and S. Aglasan (2021): "Warming temperatures, yield risk and crop insurance participation," *European Review of Agricultural Economics*, 48, 1109–1131.

Weintraub, G. Y., C. L. Benkard, and B. Van Roy (2008): "Markov perfect industry dynamics with many firms," *Econometrica*, 76, 1375–1411.

Whitt, C., K. Lacy, and K. Lim (2023): "Americas Farms and Ranches at a Glance," Accessed: 11 October 2024.

Yan, L. and D. P. Roy (2016): "Conterminous United States crop field size quantification from multi-temporal Landsat data," *Remote Sensing of Environment*, 172, 67–86.

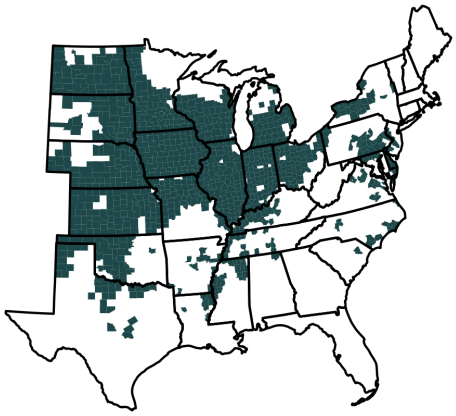
Yu, J., A. Smith, and D. A. Sumner (2018): "Effects of crop insurance premium subsidies on crop acreage," *American Journal of Agricultural Economics*, 100, 91–114.

Zulauf, C., G. Schnitkey, N. Paulson, J. Coppess, and K. Swanson (2020): "Revenue Protection: The Most Used Crop Insurance Product," Accessed: 25 September 2024.

Supplementary Material for
Protect or Prepare? Crop Insurance and Adaptation in a Changing Climate

A1 Supplemental Material: Data and Motivating Evidence

Figure A1. Selected Counties



Notes: A county is selected in the sample if (*i*) it is to the East of the 100$^{\text{th}}$ meridian, (*ii*) at least 5% of the area of the county is classified as agricultural land in the CDL for all years in the sample (2008-2020), and (*iii*) if at least 60% of the agricultural area corresponds to one of the selected 3 crop (corn, wheat, soybeans) for all years in the sample.

Table A1. Crop Insurance Subsidies 2011-2022

Coverage Level	Subsidy
0.50	0.67
0.55	0.64
0.60	0.64
0.65	0.59
0.70	0.59
0.75	0.55
0.80	0.48
0.85	0.38

Notes: Data from USDA Risk Management Agency actuarial database.

A1.1 Extreme Temperatures and Yields

Table A2. Impact of Weather on Yields by Region

Dependent Variable:	log Yields		
Crop:	Corn	Soybeans	Wheat
	(1)	(2)	(3)
Extreme Degree Days	-0.0082***	-0.0066***	-0.0010
	(0.0016)	(0.0007)	(0.0007)
Extreme Degree Days × Cooler Climate	-0.0015	-0.0023**	-0.0008
	(0.0019)	(0.0011)	(0.0012)
County FE	Yes	Yes	Yes
State-Year FE	Yes	Yes	Yes
Observations	8,075	7,757	5,753
R^2	0.86	0.87	0.87

Notes: The sample includes all counties in Appendix Figure A1 between 2011 and 2019. Extreme degree days is the number of 30° C degree days measured during the growing season, expressed in tens. Counties in the Cooler Climate group have below median number of extreme degree days. Wheat is a combination of winter and spring wheat. All specifications control for precipitation levels and the number of degree days between 10 and 30°. Standard errors are clustered at the state level. Significance levels: *** p<0.01, ** p<0.05, * p<0.1.

A1.2 Crop Insurance and Moral Hazard

Insurance may reduce farmers' incentives to exert effort in production. Because insurance take-up is also likely to be higher in locations more frequently exposed to severe weather shocks, estimated climate-yield relationships may be confounded by omitted variable bias. Following Annan and Schlenker (2015), I investigate the importance of moral hazard in my sample and estimate

$$\ln \text{Yields}^k_{mt} = \beta^k_1 \text{ExtremeDegreeDay}_{mt} + \beta^k_2 \text{ShareInsured}^k_{mt} + \beta^k_3 \text{ExtremeDegreeDay}_{mt} \times \text{ShareInsured}^k_{mt} + X^k_{mt} + \epsilon^k_{mt} \quad \text{(A1)}$$

where the dependent variable is the log of yields of crop k in county m at time t. The main parameter of interest β^k_3 captures the effect of the interaction between weather shocks—measured by the number of extreme degree days expressed in hundreds—and the share of insured planted acres. X_{mt} contains county-specific quadratic time trends, county-, year-fixed effects and controls for precipitation and the number of degree days between 10 and 30°C, as well as their interaction with the insured share. The identifying assumption is that endogenous insured share and yields are jointly independent from weather shocks.

Table A3. Effect of insurance share on crop yields

Dependent Variable:	Log Yields		
Crop:	Corn	Soybeans	Wheat
	(1)	(2)	(3)
Extreme Degree Days	-0.0046***	-0.0071***	-0.0004
	(0.0009)	(0.0007)	(0.0006)
Insured share	-0.0665	0.0379	-0.0898
	(0.0930)	(0.1284)	(0.2388)
Extreme Degree Days × Insured share	-0.0013***	0.0006	-0.0006
	(0.0004)	(0.0007)	(0.0009)
County FE	Yes	Yes	Yes
Year FE	Yes	Yes	Yes
County × Year^2	Yes	Yes	Yes
Observations	27,453	24,963	14,195
R^2	0.77076	0.77092	0.72922

Notes: Figure A1 shows the sample of included counties. Extreme degree days measure crop exposure to temperatures above 30° C during the growing season and are expressed in tens. Insured share is computed by dividing the total number of planted acres of crop k in county m in year t by the average number of planted acres of crop k between 1989 and 2019 (Annan and Schlenker, 2015). All regressions control for precipitation levels, the number of degree days between 10 and 30° and the interaction between both variables and insured share. Standard errors are clustered at the state level. Significance levels: *** p<0.01, ** p<0.05, * p<0.1.

Results are presented in Table A3 for the sample of counties included in the analysis (Figure A1). Consistent with Annan and Schlenker (2015), I find that corn yields are more sensitive to weather shocks in counties where the share of agricultural acres insured is higher. This suggests that farmers withhold effort in years when yields are negatively affected by weather shocks *and* in counties where insurance take-up is high. However, the interaction effect is smaller than the direct effect of weather shocks on yields and is smaller than estimated in Annan and Schlenker (2015). Additionally, I do not detect an effect of the interaction of weather shock and insured share on soybeans or wheat yields. Results are qualitatively and quantitatively similar when adding state-by-year fixed effects.

In a second exercise, I relax the strong identifying assumption of equation (A1) in an event-study design leveraging variation in insurance take-up encouraged by the Federal Crop Insurance Reform Act in 1994, borrowing from Havnes and Mogstad (2011).

After the passage of the Act, the insured share increased by 120% on average. I cut the sample (Figure A1) in counties above versus below the median of insurance share *growth* between 1994 and 1996. Figure A2 shows the time series of the average insured share for corn pre- and post-reform

for both groups of counties. The graphs move in parallel before the reform, with take-up highest in counties where subsequent take-up growth is lowest. The insured share in treatment counties (above median) kinks heavily after the reform, and the insured share in the two groups converges. This illustrates that the study compares counties that differ distinctly in terms of changes in insurance coverage within a narrow time frame.

Then, I study the impact of weather on crop yields pre- and post-reform in each of the two groups of counties, G_q where $q \in \{\text{above, below median}\}$. I estimate

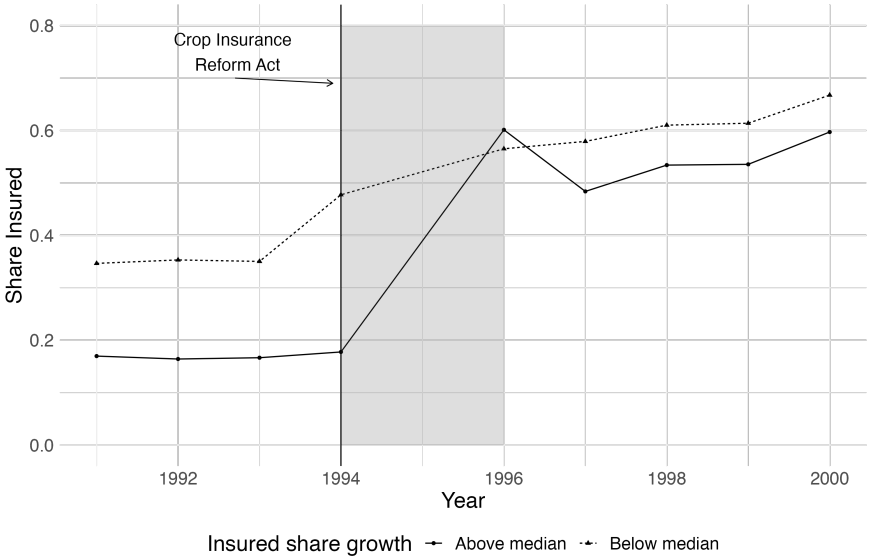
$$\ln \text{Yields}^k_{mt} = \lambda^k_1 \text{ExtremeDegreeDay}_{mt} \times \mathbf{1}[m \in G_q] + \lambda^k_2 \text{ExtremeDegreeDay}_{mt} \times \text{Post} \times \mathbf{1}[m \in G_q] + X^k_{mt} + \epsilon^k_{mt} \quad \text{(A2)}$$

where Post is a dummy equal to one if $t >= 1995$. X^k_{mt} contains county- and state-by-year-fixed effects and controls for pre- and post-reform insured shares, precipitation levels, and the number of degree days between 10 and 30°C. These controls assuage some of the concerns that the time trend in yields differs by, e.g., farmer's ability, while there are systematic differences in farmer's ability between treatment and comparison counties. Results are robust to changing the cutoff year for Post to 1996 and dropping insured share controls.

Estimation results for equation (A2) are presented in Table A4. In the pre-period, counties with a higher insurance baseline ("below") have a larger elasticity of corn yield to extreme degree days. This may be explained by selection—farmers in more vulnerable county-year insure their production at a higher rate—or moral hazard—in counties with a higher share of insurance, farmers reduce their effort. However, contrary to the moral hazard hypothesis, I do not find that counties in the "above" group see the largest increase in yield sensitivity to heat post-reform. This suggests that moral hazard does not play as large a role.

Overall, these results suggest that in counties sampled for this analysis, the RMA, which takes many precautions to audit insured farmers, successfully limits farmers' ability to decrease their efforts following insurance enrollment (see Section 2). As a result, in the rest of the paper I abstract from this channel when modeling crop insurance and land-use decisions.

Figure A2. Insured share of corn acres by treatment group



Notes: Sampled counties (Figure A1) are grouped into four quartiles of insurance adoption by corn growers following the reform of the Federal Crop Insurance Program in 1994. Counties in the first quartile see their adoption *decrease* post-reform, while counties in the fourth quartile see the largest increase in insurance take-up. Similar graphs can be produced for soybeans and wheat growers but are omitted for conciseness. Extreme degree days are measured in tens over the growing season (May-October).

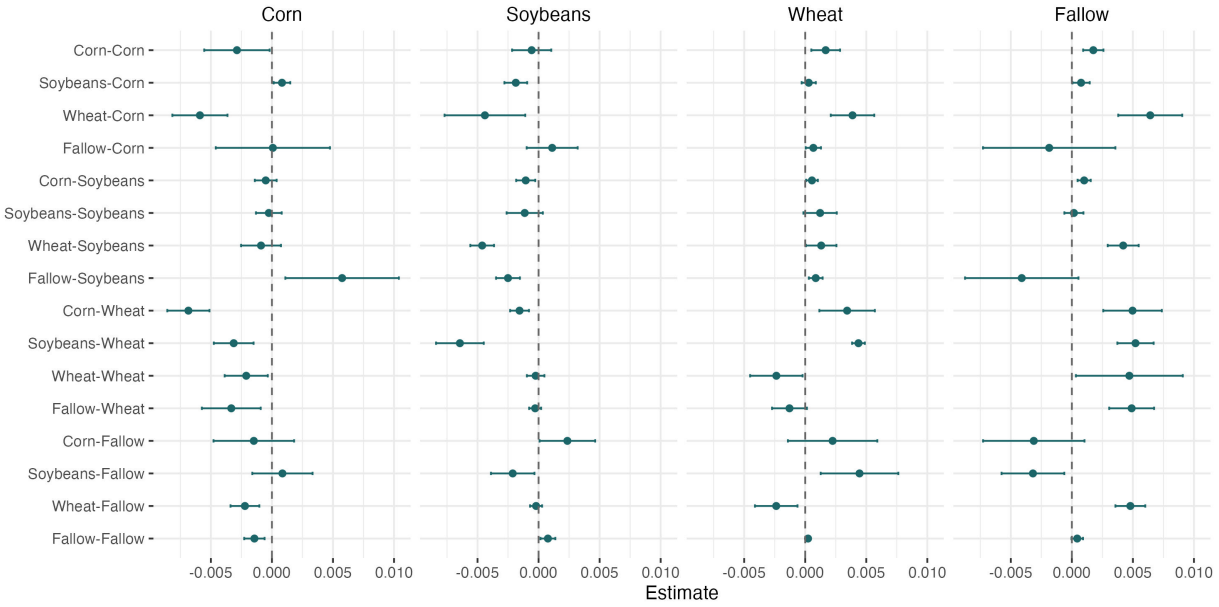
Table A4. Effect of weather shocks on yields pre- and post-insurance reform Act (1994)

Dependent Variable:	log Yields		
Crop:	Corn	Soybeans	Wheat
	(1)	(2)	(3)
Extreme Degree Day × Below	-0.0090***	-0.0100***	-0.0021**
	(0.0017)	(0.0016)	(0.0010)
Extreme Degree Day × Above	-0.0060***	-0.0075***	-0.0019**
	(0.0017)	(0.0019)	(0.0009)
Extreme Degree Day × Below × Post	0.0011	0.0032**	0.0009
	(0.0009)	(0.0013)	(0.0007)
Extreme Degree Day × Above × Post	-0.0002	0.0017	0.0002
	(0.0010)	(0.0012)	(0.0005)
County FE	Yes	Yes	Yes
State-Year FE	Yes	Yes	Yes
Observations	27,453	24,963	14,195
R^2	0.85	0.84	0.83

Notes: Counties in the sample (Figure A1) are grouped in two sets: counties above versus below the median of insurance share *growth* between 1994 and 1996 (see Figure A2). Extreme degree days measure crop exposure to temperatures above 30° C during the growing season, and is expressed in hundreds. Standard errors are clustered at the state level. Significance levels: *** p<0.01, ** p<0.05, * p<0.1.

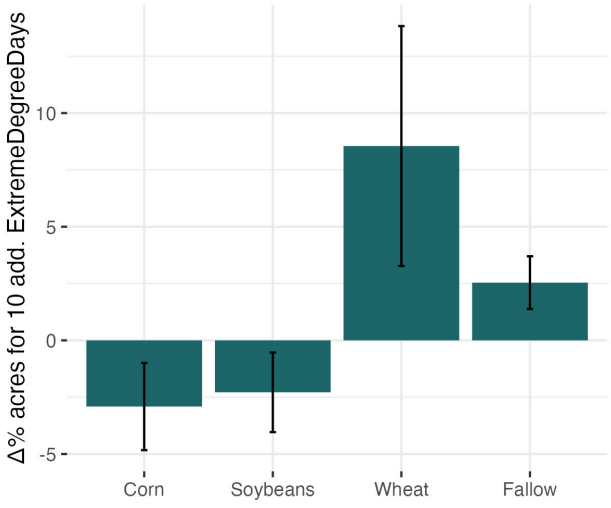
A1.3 Crop Switching and Adaptation

Figure A3. Extreme Degree Days and CCPs - Long difference



Notes: Each point represents the estimated coefficient from a regression of changes in CCPs on changes in county-level exposure to extreme degree days, using a long-difference specification comparing 2011–2014 to 2016–2019 (Equation 2). Horizontal bars denote 95% confidence intervals. The sample of counties included in the analysis is shown in Figure A1. Standard errors are clustered at the state level. Coefficients are reported separately for each crop action (columns) and each prior crop sequence (rows). Negative coefficients for corn and soybeans indicate that higher heat exposure reduces the probability of maintaining or switching into these crops, while positive coefficients for wheat and fallow suggest substitution toward cooler-season or less input-intensive alternatives.

Figure A4. Extreme Degree Days and Acres



Notes: Each bar reports the simulated percentage change in total planted acreage associated with a uniform increase of ten additional extreme degree days across all counties, based on the long-difference estimates shown in Figure A3. Error bars represent 95% confidence intervals computed from state-clustered standard errors. The results indicate significant declines in corn and soybean acreage and corresponding increases in wheat and fallow, consistent with substitution toward more heat-resistant land covers under higher heat exposure. The sample of counties included in the analysis is shown in Figure A1.

A2 Supplemental Material: Reduced-form inverse demand

The empirical and counterfactual exercises in the paper require a transparent mapping from (weather-driven) production shocks to the U.S. crop prices that enter farmers' revenues and insurance payoffs. Rather than imposing a fully specified structural demand-and-trade system, I estimate a reduced-form inverse-demand relationship that directly summarizes how equilibrium U.S. prices respond to exogenous supply movements.

For crop $k \in \{\text{corn}, \text{soybeans}, \text{wheat}\}$ and year t, let p_{kt} denote the U.S. national average price received and let Q_{kt} denote total world production (U.S. plus rest-of-world) for crop k. I estimate:

$$\ln p_t^k = \beta_k + \beta_Q \ln Q_{kt} + \nu_{kt} \tag{A3}$$

where β_k are crop fixed effects (one intercept per crop) and β_Q is the pooled elasticity of the U.S. price with respect to world production.

Identification and instruments. A key challenge is that Q_{kt} is endogenous: acreage, input use, and other supply choices respond to price expectations; additionally, measurement error in quantities mechanically biases the OLS slope. To recover the causal price response to supply shifts, I instrument $\ln Q_{kt}$ using annual growing-season weather realizations. The identifying assumption is standard in agricultural commodity markets: weather affects equilibrium prices primarily through its effect on yields and hence production, while being orthogonal to contemporaneous demand shocks.

This strategy is closely related to the approach in Roberts and Schlenker (2013), who identify supply and demand elasticities for major staple crops using yield shocks that are predominantly driven by weather. More broadly, the use of weather as an exogenous supply shifter to identify agricultural demand relationships has a long tradition in this literature.

Concretely, I estimate (A3) by 2SLS using a first stage of the form:

$$\ln Q_{kt} = \delta_k + \Pi' Z_{kt} + \mu_{kt}, \tag{A4}$$

where Z_{kt} includes area-weighted growing-season precipitation and temperature measures (e.g., precipitation, minimum temperature, and maximum temperature) constructed to reflect conditions

in major producing regions for crop k in year t.[31]

Why a reduced-form approach? The goal of the crop-demand block in this paper is not to interpret primitive preferences or to separately identify trade and storage mechanisms. Instead, the model requires a *stable, data-consistent price process* that maps plausibly exogenous supply variation into the U.S. prices relevant for farm incomes and insurance.

Estimating (A3) by weather-based IV has two advantages for this purpose. First, it is tightly linked to the source of identifying variation emphasized in the literature: weather shocks generate quasi-random movements in yields and quantities that shift supply and therefore equilibrium prices (Roberts and Schlenker, 2013). Second, because (A3) is a reduced-form equilibrium relationship, the estimated β_Q implicitly aggregates all adjustment margins that connect world quantities to U.S. prices—including trade reallocation, inventory behavior, and other market responses—without requiring the model to explicitly parameterize each margin.

Results. Table A5 reports pooled estimates of (A3). Column (1) shows the pooled OLS relationship between log prices and log world production, controlling for crop fixed effects. The OLS slope is small and statistically indistinguishable from zero, consistent with endogeneity from supply responses to expected prices. Column (2) reports the preferred 2SLS estimates that instrument $\ln Q_{kt}$ with growing-season weather. The IV estimate implies a precisely estimated inverse-demand elasticity equal to -0.356. The first-stage F-statistic for the excluded instruments is 31.9, indicating strong predictive power of the weather instruments for production in this sample. This estimate implies a 10% increase in production is associated with a 3.6% decline in the U.S. price. This magnitude can be interpreted as a reduced-form price flexibility that aggregates multiple equilibrium adjustment margins (trade reallocation, inventory behavior, and substitution across uses), and is therefore expected to be smaller in absolute value than short-run flexibilities estimated from high-frequency supply news. For example, using monthly revisions to USDA crop forecasts, Adjemian and Smith (2012) estimate own-commodity demand flexibilities of about -1.35 for corn and -1.03 for soybeans at average inventories. Consistent with this comparison, restricting attention to U.S. production only increases the estimated elasticity in absolute value ($\widehat{\beta}_Q = -0.629$, see Columns (3) and (4) in Table A5), bringing it closer to these benchmarks by removing dilution from contemporaneous variation in foreign production. Finally, allowing elasticities to differ by crop yields a

[31] In practice, I use annual summaries of growing-season weather from gridded climate products and aggregate them using crop-specific harvested-area weights.

Table A5. Estimated Crop Demand Parameters

Dependent Variable:	log Price			
Production:	Worldwide		U.S. only	
	(1)	(2)	(3)	(4)
β^{Corn}	5.426***	7.683***	5.887***	8.415***
	(0.4649)	(0.6634)	(0.4125)	(0.8895)
β^{Soybeans}	6.191***	8.031***	6.528***	8.490***
	(0.3816)	(0.5404)	(0.3233)	(0.6860)
β^{Wheat}	5.660***	7.890***	5.868***	7.719***
	(0.4647)	(0.6625)	(0.3082)	(0.6547)
β^{Q}	-0.0652	-0.3559***	-0.1741**	-0.6291***
	(0.0604)	(0.0858)	(0.0753)	(0.1600)
Observations	105	105	105	105
R^2	0.68	0.64	0.69	0.63
F-test (1st stage)		31.87		14.89

Notes: This table reports estimates from the pooled 2SLS specification in (A3) using annual data for 1985–2019 and crops $k \in \{\text{corn}, \text{soybeans}, \text{wheat}\}$. The dependent variable is the log U.S. national average price received for crop k. The endogenous regressor is log world production Q_{kt} (U.S. plus rest-of-world). Instruments are area-weighted growing-season weather measures (precipitation and temperature) as in (A4). The reported crop intercepts $\{\beta_k\}$ correspond to crop fixed effects (with no common constant), and β_Q is the pooled elasticity of price with respect to production. Standard errors are robust. Significance levels: *** p<0.01, ** p<0.05, * p<0.1.

coherent pattern (Table A6): corn and soybeans exhibit relatively similar and low price flexibility (-0.29 and -0.24), while wheat is more price responsive (-0.86), consistent with wheat having broader substitution possibilities and more globally integrated arbitrage.

Figure A5 visualizes model fit by comparing predicted and observed prices in levels. The log-linear specification with crop fixed effects matches the cross-crop average price levels and captures a substantial fraction of within-crop time-series variation, while compressing the most extreme realizations, which is typical in parsimonious log-linear mappings and helps stabilize counterfactual price simulations.

Implementation in counterfactual simulations. For any counterfactual production path $\{Q_{kt}^{cf}\}$, I generate predicted prices using:

$$\widehat{\ln p_t^k}^{\,cf} = \widehat{\beta}_k + \widehat{\beta}_Q \ln Q_{kt}^{cf}. \tag{A5}$$

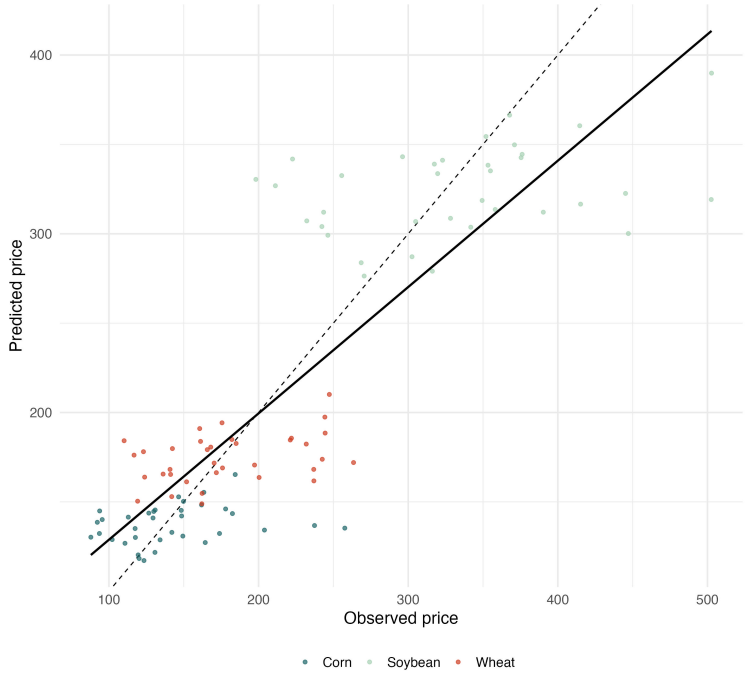
Table A6. Estimated Crop Demand Parameters by Crop

Dependent Variable:	log Price		
Crop:	Corn	Soybeans	Wheat
	(1)	(2)	(3)
β_k	7.181***	7.265***	11.76***
	(0.8181)	(0.6388)	(2.643)
β^Q	-0.2913***	-0.2348**	-0.8596**
	(0.1061)	(0.1011)	(0.3439)
Observations	35	35	35
F-test (1st stage)	15.110	13.259	13.382

Notes: This table reports estimates from the pooled 2SLS specification in (A3) using annual data for 1985–2019 and crops $k \in \{\text{corn}, \text{soybeans}, \text{wheat}\}$. The dependent variable is the log U.S. national average price received for crop k. The endogenous regressor is log world production Q_{kt} (U.S. plus rest-of-world). Instruments are area-weighted growing-season weather measures (precipitation and temperature) as in (A4). The reported crop intercepts $\{\beta_k\}$ correspond to crop fixed effects, and β_Q is the crop-specific elasticity of price with respect to production. Standard errors are robust. Significance levels: *** p<0.01, ** p<0.05, * p<0.1.

To preserve the empirical dispersion of prices within each crop, I also compute crop-specific residual standard deviations $\widehat{\sigma}_k = sd(\widehat{\nu}_{kt} \mid k)$ from (A3) and use these moments when simulating idiosyncratic price shocks in counterfactuals.

Figure A5. Crop Demand Model Fit



Notes: The figure plots model-predicted prices against observed U.S. prices for 1985–2019, by crop.

A3 Supplemental Material: Crop Insurance Demand Estimation

A3.1 Insurance Characteristics

During the pre-planting season, farmers form beliefs about end-of-season yields and crop prices. When combined with the design of the crop insurance program, these beliefs determine the characteristics of the available insurance plans, $\Delta\mathbb{E}$ and ΔVar. Farmers use those characteristics to decide whether to insure their production and how much coverage to purchase.

A3.1.1 County-level Yield Beliefs

Realized yield distributions. For each county m, year t, crop k, and coverage level x, I observe the number of yield-protection policies sold $n(x)$ and the number of policies claiming indemnities $n^{\text{ind}}(x)$. Since indemnities occur when realized yields fall below $x \cdot \overline{\text{Yield}}_{mkt}$, these counts contain information about the lower-tail probability mass of the yield distribution.

I assume yields are lognormally distributed, $\text{Yield}_{mkt} \sim \text{LN}(\mu_{mkt}, \sigma^2_{mkt})$. Anchoring the mean at the USDA county-year mean $\overline{\text{Yield}}_{mkt}$ implies

$$\mu_{mkt} \;=\; \log\!\big(\overline{\text{Yield}}_{mkt}\big) \;-\; \tfrac{1}{2}\sigma^2_{mkt}.$$

For a coverage threshold $x \in \mathcal{X}_{mkt}$ (the set of coverage levels sold in that county-year), the indemnity probability is

$$p_x(\sigma_{mkt}) \;=\; \Pr\!\big(\text{Yield}_{mkt} \le x\,\overline{\text{Yield}}_{mkt}\big) \;=\; \Phi\!\left(\frac{\log(x\,\overline{\text{Yield}}_{mkt}) - \mu_{mkt}}{\sigma_{mkt}}\right),$$

where $\Phi(\cdot)$ is the standard normal CDF. The observed indemnity counts are then binomial:

$$n^{\text{ind}}(x) \mid \sigma_{mkt} \;\sim\; \text{Binomial}\big(n(x),\, p_x(\sigma_{mkt})\big)\,,$$

giving the likelihood

$$\mathcal{L}\Big(\{n^{\text{ind}}(x)\}_x \mid \sigma_{mkt}\Big) = \prod_{x\in\mathcal{X}_{mkt}} \big[p_x(\sigma_{mkt})\big]^{n^{\text{ind}}(x)} \big[1 - p_x(\sigma_{mkt})\big]^{\,n(x)-n^{\text{ind}}(x)}.$$

I place an inverse gamma prior on the variance of log yields, denote its distribution by $f_{InvGamma}$

and obtain the county-year-crop estimate by Maximum A Posteriori estimation:

$$\hat{\sigma}_{mkt} \;=\; \arg\max_{\sigma_{mkt}>0} \; \mathcal{L}\Big(\{n^{\text{ind}}(x)\}_x \mid \sigma_{mkt}\Big) \;\times\; f_{InvGamma}\Big(\sigma^2_{mkt}\Big)\,.$$

Climate beliefs. I assume farmers form expectations of growing-season weather using pre-planting conditions and past realizations. I estimate linear forecasting models for extreme degree days (> 30°C), degree days (10–30°C), and precipitation using PRISM (1985-2020):

$$\text{ExtremeDegreeDay}^{GS}_{mt} = f^{EDD}(\text{Climate}^{PS}_{mt}, \text{Climate}^{GS}_{mt-1}) + X_m + \nu_{1mt} \tag{A6}$$

$$\text{DegreeDay1030}^{GS}_{mt} = f^{DD}(\text{Climate}^{PS}_{mt}, \text{Climate}^{GS}_{mt-1}) + X_m + \nu_{2mt} \tag{A7}$$

$$\text{Precipitation}^{GS}_{mt} = f^{prec}(\text{Climate}^{PS}_{mt}, \text{Climate}^{GS}_{mt-1}) + X_m + \nu_{3mt} \tag{A8}$$

where Climate collects precipitation, degree days (10-30°C), and extreme degree days (> 30°C), and X_m includes elevation and ruggedness. These parsimonious models explain a large share of variation in growing-season weather outcomes (74% for extreme temperatures, 52% for precipitation; Table A7). The residual vector $(\nu_{1mt}, \nu_{2mt}, \nu_{3mt})$ is allowed to be jointly correlated. I use its empirical covariance matrix with the parameters in Table A7 to simulate weather belief draws.

Yield models. I relate moments of realized yields to growing-season weather via

$$\ln \text{Yield}^{k}_{mt} = \boldsymbol{\beta}^{k} \times \text{Climate}^{GS}_{mt} + \alpha_m + \alpha_t + \epsilon^{k}_{mt} \tag{A9}$$

$$\ln \text{sd(Yields)}^{k}_{mt} = \boldsymbol{\beta}^{k,V} \times \text{Climate}^{GS}_{mt} + \alpha_m + \alpha_t + \epsilon^{kV}_{mt} \tag{A10}$$

where where Climate includes precipitation, growing degree days (10-30°C), and extreme degree days (>30°C), α_m and α_t are county and time fixed effects. Results are shown in Table A8.

Yield beliefs. For each simulated draw from farmers' weather beliefs $\tilde{w}$, I use the estimated yield models (Equations A9–A10) to obtain two conditional moments: the conditional mean of log yields and the conditional standard deviation of yields in levels,

$$\mu(\tilde{w}) = \mathbb{E}[\ln \text{Yield} \mid \tilde{w}], \qquad s(\tilde{w}) = \text{sd}[\text{Yield} \mid \tilde{w}].$$

Table A7. Weather forecasting models

Climate moment	Extreme degree day^{GS}	Growing degree day^{GS}	Precipitation^{GS}
	(1)	(2)	(3)
Precipitation^{PS}	-0.0459***	-0.0641***	0.4072***
	(0.0012)	(0.0061)	(0.0086)
Extreme degree day^{PS}	12.18***	8.588***	-17.58***
	(0.7407)	(1.164)	(1.652)
Growing degree day^{GS}	0.0338***	0.5195***	0.2903***
	(0.0023)	(0.0100)	(0.0130)
Lag precipitation^{GS}	0.0117***	0.1439***	0.4166***
	(0.0006)	(0.0035)	(0.0044)
Lag extreme degree day^{GS}	0.6205***	0.0024	-0.3869***
	(0.0083)	(0.0177)	(0.0214)
Lag growing degree day^{GS}	0.0191***	0.8668***	-0.0186***
	(0.0005)	(0.0022)	(0.0025)
Observations	77,550	77,550	77,550
R^2	0.73833	0.94116	0.51756

Notes: Models estimated on counties in Figure A1, using PRISM data (1985-2020). All specifications include elevation and ruggedness. Standard errors are robust. Significance levels: *** $p < 0.01$, ** $p < 0.05$, * $p < 0.1$.

To recover the log-variance $\sigma^2(\tilde{w})$ from the level standard deviation $s(\tilde{w})$, note that lognormal moments imply

$$s(\tilde{w}) = \sqrt{\exp\big(2\mu(\tilde{w})\big)\Big(\exp\big(2\sigma^2(\tilde{w})\big) - \exp\big(\sigma^2(\tilde{w})\big)\Big)}.$$

Let $A(\tilde{w}) \equiv s^2(\tilde{w})\exp(-2\mu(\tilde{w}))$ and define $z(\tilde{w}) \equiv \exp(\sigma^2(\tilde{w}))$. Then $A(\tilde{w}) = z^2(\tilde{w}) - z(\tilde{w})$, implying

$$z(\tilde{w}) = \frac{1 + \sqrt{1 + 4A(\tilde{w})}}{2}, \qquad \sigma^2(\tilde{w}) = \log z(\tilde{w}).$$

Given $\mu(\tilde{w})$ and $\sigma^2(\tilde{w})$, the first two conditional moments in levels are

$$\mathbb{E}[\text{Yield} \mid \tilde{w}] = \exp\big(\mu(\tilde{w}) + \tfrac{1}{2}\sigma^2(\tilde{w})\big), \qquad \mathbb{E}[\text{Yield}^2 \mid \tilde{w}] = \exp\big(2\mu(\tilde{w}) + 2\sigma^2(\tilde{w})\big).$$

Finally, integrating over weather uncertainty yields planting-time moments

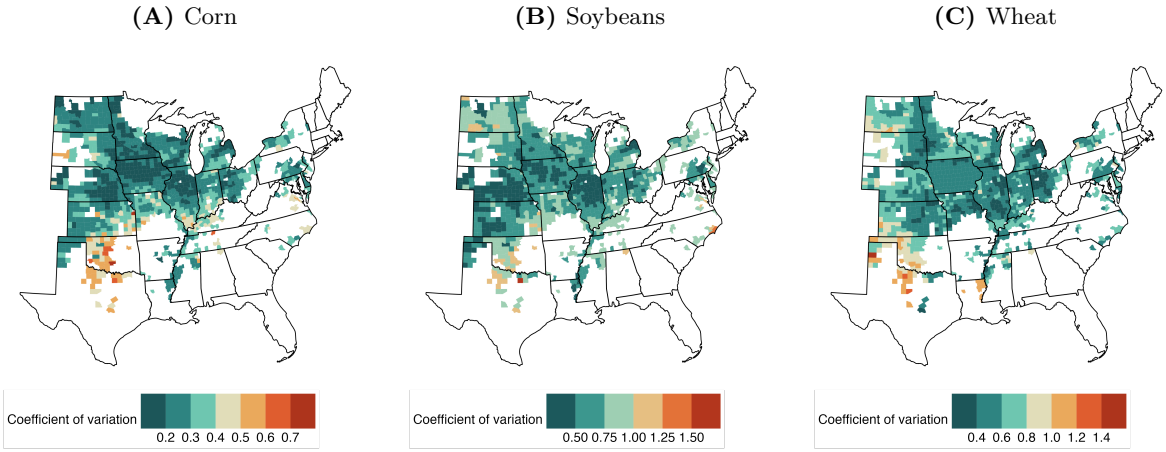
$$M_1 \equiv \mathbb{E}_{\tilde{w}}[\mathbb{E}[\text{Yield} \mid \tilde{w}]], \qquad M_2 \equiv \mathbb{E}_{\tilde{w}}\Big[\mathbb{E}[\text{Yield}^2 \mid \tilde{w}]\Big],$$

Table A8. Models of yields average and standard deviation

Crop:	Corn	Soybeans	Wheat
	(1)	(2)	(3)
Panel A: Log Mean Yield			
Extreme Degree Days	-0.0067***	-0.0060***	-0.0005
	(0.0011)	(0.0004)	(0.0004)
Growing Degree Days	0.0005**	-1.16×10^{-5}	-0.0007**
	(0.0002)	(8.47×10^{-5})	(0.0003)
Precipitation	3×10^{-5}	3.22×10^{-5}	$-9.96 \times 10^{-5*}$
	(5.44×10^{-5})	(5.64×10^{-5})	(5.47×10^{-5})
County FE	Yes	Yes	Yes
Year FE	Yes	Yes	Yes
Observations	8,075	7,757	5,753
R^2	0.76734	0.81231	0.79253
Panel B: Log Sd. Yield			
Extreme Degree Days	0.0051***	0.0043***	0.0004
	(0.0007)	(0.0008)	(0.0002)
Growing Degree Days	-6.13×10^{-5}	0.0001	0.0007**
	(0.0002)	(0.0001)	(0.0003)
Precipitation	0.0001***	0.0001***	$9.84 \times 10^{-5**}$
	(4.63×10^{-5})	(4.56×10^{-5})	(4.67×10^{-5})
County FE	Yes	Yes	Yes
Year FE	Yes	Yes	Yes
Observations	8,049	7,729	5,734
R^2	0.80602	0.85512	0.80426

Notes: Models estimated on counties in Figure A1, using PRISM data (1985-2020). All specifications include elevation and ruggedness. Standard errors are clustered at the state level. Significance levels: *** $p < 0.01$, ** $p < 0.05$, * $p < 0.1$. The sample includes all counties in Appendix Figure A1 between 2011 and 2019. Extreme degree days is the number of 30° C degree days measured during the growing season, expressed in tens. Growing degree days is the number of 10–30°C degree days measured over the growing season, expressed in tens. Precipitation in measured over the growing season and is measured in mm. Wheat is a combination of winter and spring wheat. Standard errors are clustered at the state-year level. Significance levels: *** p<0.01, ** p<0.05, * p<0.1.

Figure A6. Pre-planting Beliefs on Yields Risk



Notes: The coefficient of variation is the ratio of standard deviation and the mean of the yield distribution. The maps plot the average of coefficient of variation for the three crop included in the analysis between 2011 and 2019. The spatial heterogeneity in corn yield risk is comparable to USDA measurements (Harwood et al., 1999).

which I summarize with a lognormal distribution matched to (M_1, M_2):

$$\sigma^{2*} = \log\left(\frac{M_2}{M_1^2}\right), \qquad \mu^* = \log(M_1) - \tfrac{1}{2}\sigma^{2*}.$$

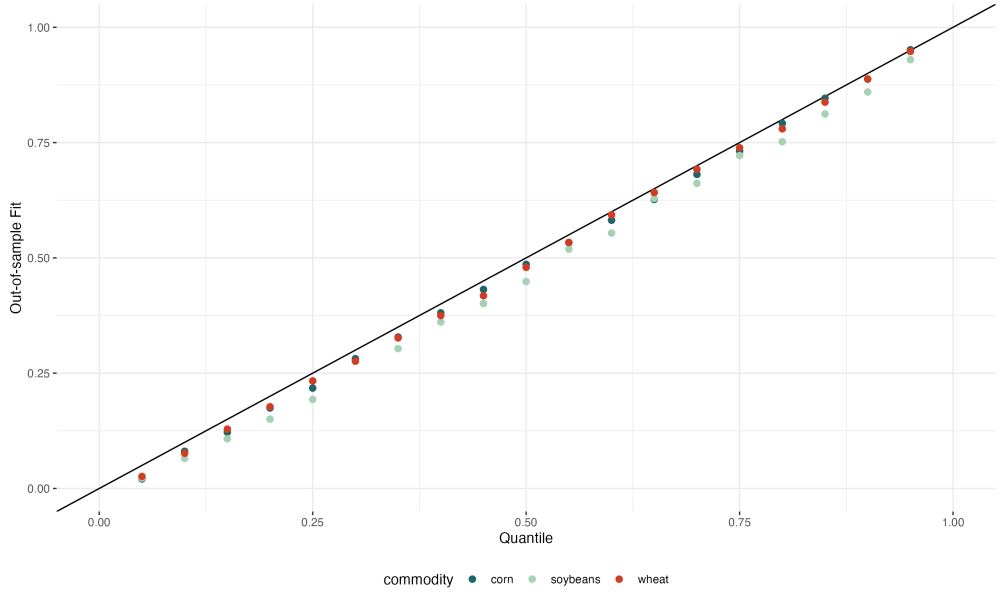
These parameters define the subjective (planting-time) yield distribution, integrating both uncertainty about growing-season weather and the estimated sensitivity of yields to climate conditions.

Validation. The resulting planting-time yield beliefs reproduce well-known features of U.S. agricultural production risk. Figure A6 maps the coefficient of variation implied by the belief distributions and shows the familiar spatial gradient: risk is lowest in the core of the Midwest and rises toward the southern and eastern fringes of the Corn Belt. This pattern closely mirrors USDA estimates of county-level corn yield variability (Harwood et al., 1999). Although the beliefs inevitably smooth some extreme tail outcomes, they capture the broad spatial structure of production risk that farmers face at planting. This provides reassurance that the yield-belief distributions used in the insurance demand estimation and counterfactual simulations are grounded in empirically realistic heterogeneity across crops and regions.

A3.1.2 Crop Price Beliefs

Farmers form beliefs on crop prices based on crop futures published during the pre-planting season. To estimate the model, I assume that farmers' beliefs are stationary and can be derived from prices of crop futures. Moreover, I assume crop prices are homogeneous across space. I recover farmers'

Figure A7. Crop Price Beliefs - Out-of-sample fit



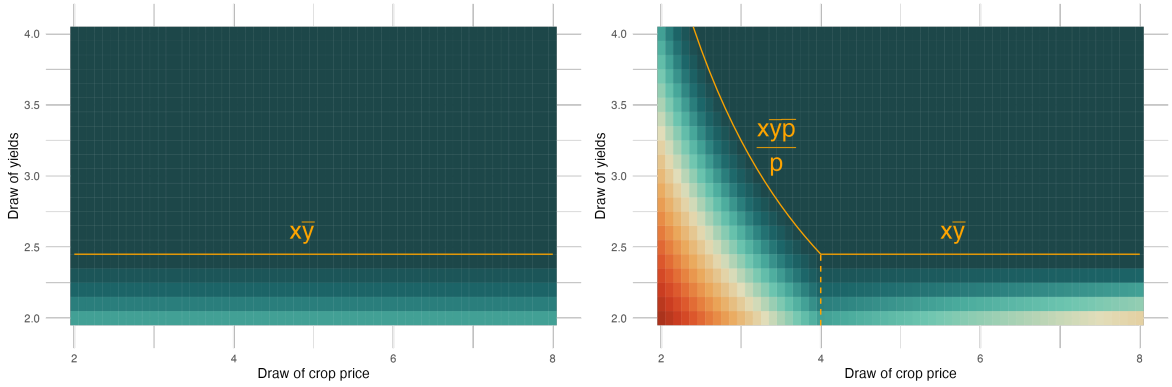
Notes: Calibration of the crop-price distribution prediction using quantile random forest. The regressors are future prices available to farmers pre-planting. The distributions of corn, soybeans, and wheat prices are overall well-calibrated: around 50% of the observations of state-level crop-specific prices over 2007-2019 fall below the estimated 50th percentile for that crop-year-state combination.

beliefs using quantile random forests (Athey, Tibshirani, and Wager, 2019). Figure A7 shows the out-of-sample fit of each quantile of the price distribution. The distributions of corn, soybeans, and wheat prices are well-calibrated. For example, 10% of the observations of corn prices over 2007-2019 fall below the estimated 10th percentile of the corn price distribution. I assume the beliefs on crop price distribution are the same between high- and low-quality farmers.

A3.1.3 Premiums

I combine farmers' beliefs about yield and crop-price distributions with insurance indemnities formulas (Figure A8) to compute actuarially fair premiums for each county–year–crop–coverage combination. I then apply the status quo subsidies shown in Table A1. Figure A9 compares these predicted premiums to the average paid premiums reported in RMA data (RMA, 2023). The model captures both the level and cross-sectional variation in premiums remarkably well: points lie close to the 45° line for all three crops, and the slope of the relationship between observed and predicted premiums is close to one. Regressing estimated premiums on paid premiums yields coefficients between 0.74 and 0.91 across crops (0.85 in the pooled sample), indicating a tight linear relationship. Corn and soybeans exhibit the strongest alignment, consistent with the richer

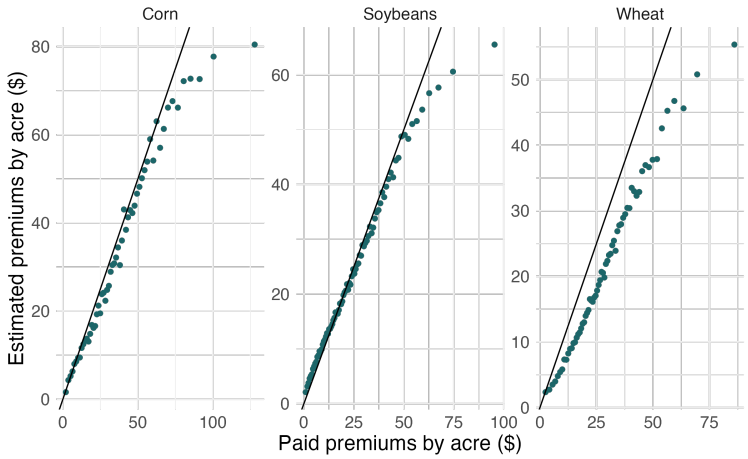
Figure A8. Illustration of Insurance Indemnities



(A) Yield Protection **(B)** Revenue Protection

Notes: Simulated indemnity schedules under Yield (Panel a) and Revenue Protection (Panel b). When subscribing to insurance, farmers choose between Yield and Revenue Protection, each subdivided into eight levels of coverage x. Combined with historical yields $\bar{y}$ and projected prices $\bar{p}$ –known at the time of subscription–, these insurance plans result in different indemnity schedules. For exposition, I use $\bar{y} = 3$, $x = 0.8$ and $\bar{p} = 4$. If realizations of yield y and price p fall below the solid black line, farmers are eligible for indemnities. In the case of Revenue Protection, the guaranteed revenue is computed using the maximum between the price at the time of harvest and the projected price: the indemnity schedule differs to the left and the right of the dashed line ($p = \bar{p}$).

Figure A9. Observed versus estimated premiums

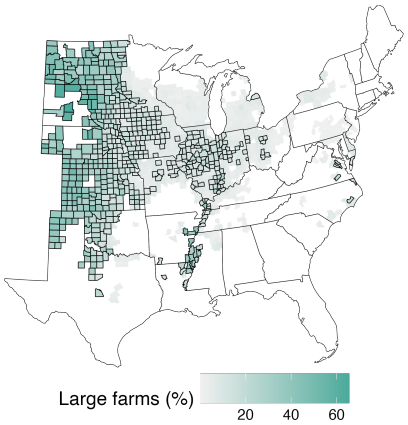


Notes: The figure plots, for each crop, the binned regression of the subsidized actuarially fair premiums implied by farmers' yield and price beliefs against observed average paid premiums per acre (RMA, 2023). Observations are at the county–year–coverage level, pooling all insurance products (Yield Protection, Revenue Protection) and all available coverage levels. The 45-degree line is shown for reference. Estimated premiums closely track paid premiums on average, indicating that the belief-based model reproduces the cross-sectional variation in actuarial risk priced by USDA RMA.

indemnity data available for these crops, while wheat shows slightly more dispersion. Some differences are expected because paid premiums embed administrative loadings, county-specific rating adjustments, and federal subsidy rates that are not modeled explicitly. Overall, the close match between estimated and observed premiums provides strong validation that the belief distributions constructed in the previous sections generate empirically realistic actuarial values.

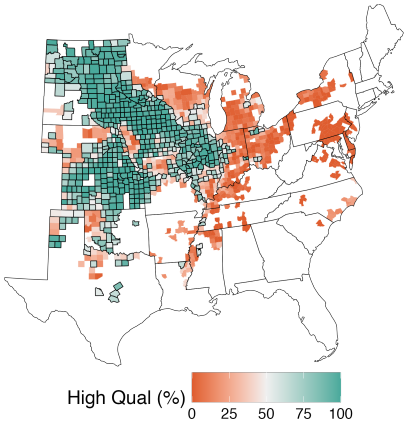
A3.2 Crop Insurance Demand Results

Figure A10. Counties with a High Share of Large Farms



Notes: Data was obtained from the U.S. Census of Agriculture in 2012. Large farms have 1000 acres or more. Outlined counties are those that have an above median share of large farms.

Figure A11. Counties with High-quality Land



Notes: Data was obtained from Soil Survey Staff (2024). The land quality map is a function of time-invariant characteristics such as soil type, elevation, and ruggedness. The index ranges from 0 to 19. I select the median quality threshold and aggregate this index into two levels (High/Low). Outlined counties are those that have an above median share of high quality land.

Table A9. Crop Insurance Demand Estimates - Robustness

Dependent Variable:	$\ln \sigma^k_{jmt}/\sigma^k_{0mt}$			
Sample:	Large farms	Small farms	High-quality land	Low-quality land
	(1)	(2)	(3)	(4)
$\Delta \mathbb{E}^k_{jtm}$	7.650***	5.755***	8.065***	4.632***
	(0.5205)	(0.5178)	(0.4974)	(0.5123)
ΔVar^k_{jtm}	-51.23***	-39.61***	-56.36***	-38.34***
	(3.165)	(2.410)	(3.615)	(2.400)
County-Crop FE	Yes	Yes	Yes	Yes
Year-Crop FE	Yes	Yes	Yes	Yes
Observations	177,905	192,491	183,821	186,575
R^2	0.258	0.173	0.254	0.181
Implied CARA (per 1,000$)	13.39	13.76	13.98	16.55
Implied RRA at outside option	4.93	5.07	5.15	6.10

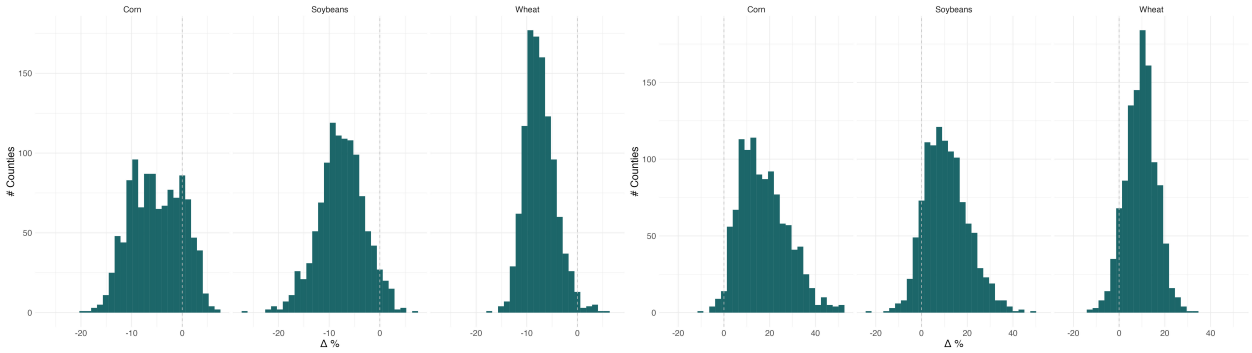
Notes: The table presents the results from the estimation of crop insurance demand on various sub-samples of counties between 2011 and 2019. Model 1 is estimated on the sample of counties with an above median share of large farms (outlined in Figure A10) Model 2 is estimated on the remaining half of counties. Model 3 is estimated on the sample of counties with an above median share of high-quality land (outlined in Figure A11). Model 4 is estimated on the remaining half of counties. Standard errors are clustered by state-year. Significance levels: *** p<0.01, ** p<0.05, * p<0.1.

A4 Supplemental Material: Dynamic Crop Choice

This appendix documents the construction of the belief objects and the solution and estimation steps for the dynamic crop choice model. I estimate the dynamic model by maximum likelihood using a nested fixed point (NFXP) algorithm (Rust, 1987). NFXP requires solving the farmer's dynamic program for each candidate parameter vector and, therefore, evaluating expected payoffs off the realized path over the model's full state space. Additionally, because the system is off steady state due to climate change, the dynamic estimation requires evaluating expected payoffs in future states of climate. I compute these payoffs for all years between 2016 and 2050.

Section A4.1 constructs yield and price beliefs under climate change, validates them in-sample, and maps beliefs into the insurance inclusive value and into $\mathbb{E}^*_{kmt}$. Section A4.2 describes the NFXP solution and estimation procedure and summarizes additional model-fit and elasticity results.

Figure A12. Change in yield beliefs 2020–2050



(A) Average **(B)** Standard deviation

Notes: The figure shows the distribution of county-level change in the average and standard deviation of crop yields between 2015-2020 and 2045-2050. Climate evolves as projected by six general circulation models under a moderate emission scenario (RCP 4.5). The sample is restricted to counties shown in Figure A1.

A4.1 Beliefs and payoff objects for the dynamic model (2016–2050)

A4.1.1 County-level yields beliefs

I rely on daily temperature and precipitation projections from six global climate models under the Representative Concentration Pathway 4.5 (RCP 4.5), a medium stabilization scenario in which greenhouse gas emissions are projected to peak around 2050 and subsequently decline. The GCMs used are ACCESS1-0, BNU-ESM, CCSM4, CESM1-BGC, MIROC_ESM, and NorESM1-M. Using multiple models smooths interannual variation in projected climate and mitigates model-specific drift.

Farmers' beliefs about yields coincide with the GCM-implied distributions over 2016–2050. For each county m, year t, and crop k, I compute farmers' planting-time beliefs by simulating weather and propagating it through the estimated yield models. Using the forecasting equations in (A6)–(A8), I construct pre-planting beliefs over growing-season weather. I simulate correlated forecast errors with the empirical covariance of $(\nu_{1mt}, \nu_{2mt}, \nu_{3mt})$ to generate a set of weather draws $\tilde{w}$ for each (m, t). I then use the same procedure as the one described in Section A3.1.1: I recover log-normal yield beliefs and draw from that belief distribution, censoring implausibly high yields (above 10 tons per acre).

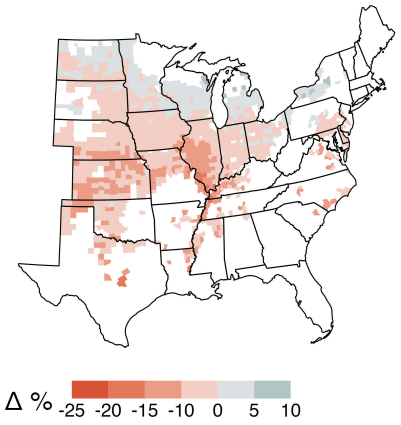
Figure A12 Panel A documents substantial climate-driven declines in average yields between 2015–2020 and 2045–2050. Farmers in most counties expect decreases in productivity, around 7% on average. These declines reflect the projected increase in the frequency and intensity of extreme

heat events under RCP 4.5. The geographic distribution of impacts is highly heterogeneous across crops: southern and central counties experience the sharpest reductions in corn and soybeans yields, whereas northern counties—particularly in the upper Midwest—see more modest declines (Figure A13). Wheat yields losses are concentrated in the Corn Belt.

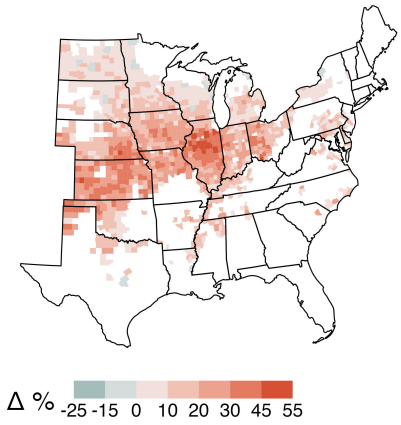
Climate change also increases production risk. Figure A12 Panel B shows the standard deviation of planting-time yield beliefs rises across nearly all counties and crops, with especially pronounced increases for corn and soybeans. The spatial maps in Figure A13 reveal a broad band of heightened variance stretching across the Corn Belt, indicating that the regions that currently produce the bulk of U.S. corn and soybeans are also those projected to experience the largest rise in yield uncertainty. Taken together, these patterns imply that future climate conditions simultaneously depress average yields and raise production risk, particularly for heat-sensitive crops and in regions already operating near agronomic temperature thresholds.

Comparison with yield beliefs in static estimation. Figure A14 compares the yield-belief distributions used in estimation (see Appendix A3.1.1) with the counterfactual yield beliefs generated under the climate-model simulations. For comparability, I focus on year 2019. Panel (a) shows that the counterfactual mean-yield beliefs lie close to the 45-degree line for all three crops, indicating that the yield models calibrated on historical weather perform well when evaluated at the climate conditions observed in 2019. Panel (b) shows a similar pattern for the standard deviation of planting-time yield beliefs, with counterfactual variability aligning closely with the variability implied by the reduced-form yield-risk model. The small deviations from the 45-degree line reflect differences in underlying weather distributions.

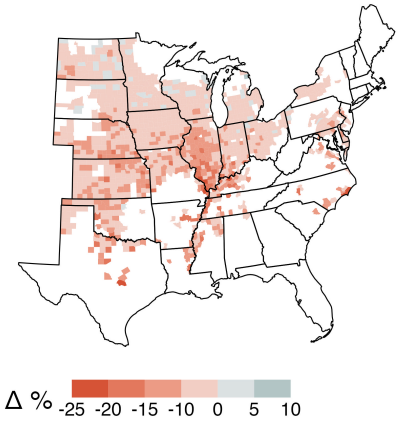
Figure A13. Change in yield beliefs across space 2020–2050



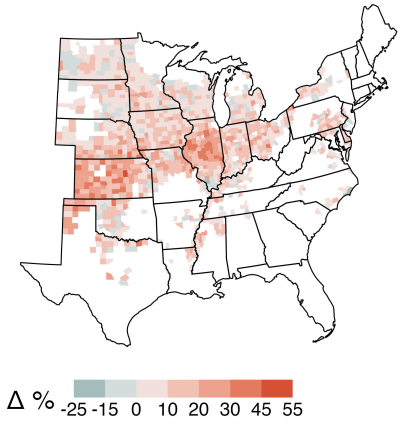
(A) Corn - Average



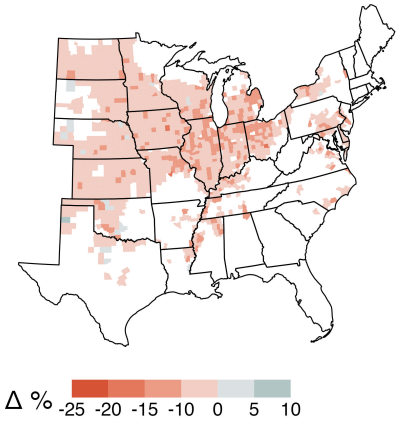
(B) Corn - Standard Deviation



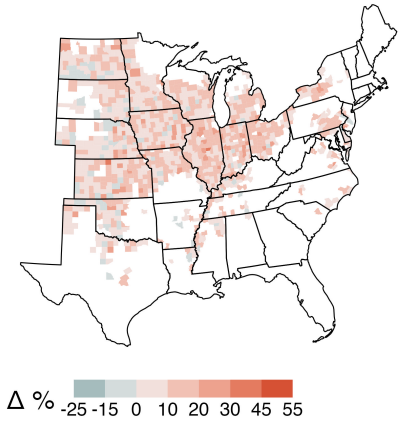
(C) Soybeans - Average



(D) Soybeans - Standard Deviation



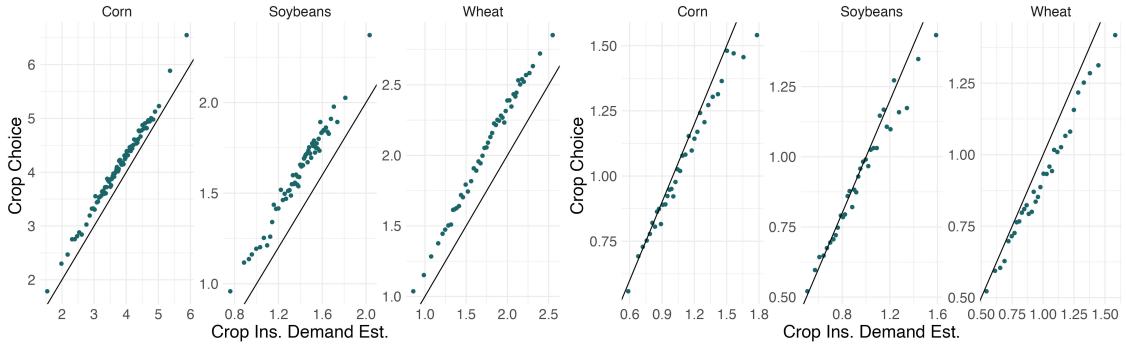
(E) Wheat - Average



(F) Wheat - Standard Deviation

Notes: The maps show the spatial distribution of county-level change in the average and standard deviation of crop yields between 2015-2020 and 2045-2050. Climate evolves as projected by six general circulation models under a moderate emission scenario (RCP 4.5).

Figure A14. Crop Yield Beliefs - Static versus Dynamic Estimation



(A) Average **(B)** Standard deviation

Notes: The figures show the results of binned regressions. The underlying data is at the a county–crop level in 2016. The horizontal axis shows the average (Panel A) or standard deviation (Panel B) of planting-time yield beliefs used in the estimation of the crop insurance demand system (see Section A3.1.1). The vertical axis shows the corresponding yield beliefs generated from the combination of yield models and climate models, used in the estimation of the dynamic crop choice model. The 45-degree line is shown for reference.

A4.1.2 Crop Price Beliefs

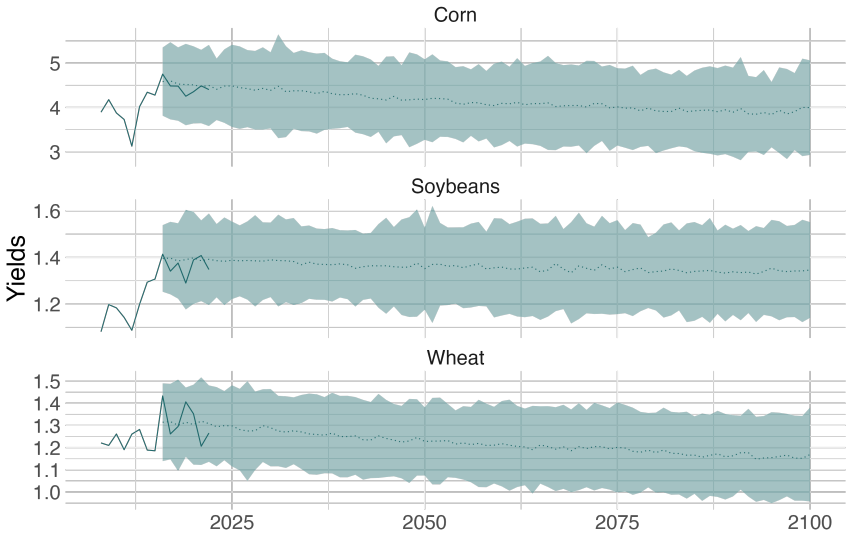
The dynamic model requires, for each year t and each aggregate acreage state s_t, planting-time beliefs about harvest prices for the three marketed crops (corn, soybeans, wheat).

The price-belief construction combines four inputs: (i) harvested areas outside the modeled counties (held fixed at their historical average), (ii) the crop demand system in Appendix A2, (iii) a grid of possible aggregate acreage allocations for the modeled U.S. counties (the discrete state s_t), and (iv) draws of projected U.S. and foreign yields for each crop.

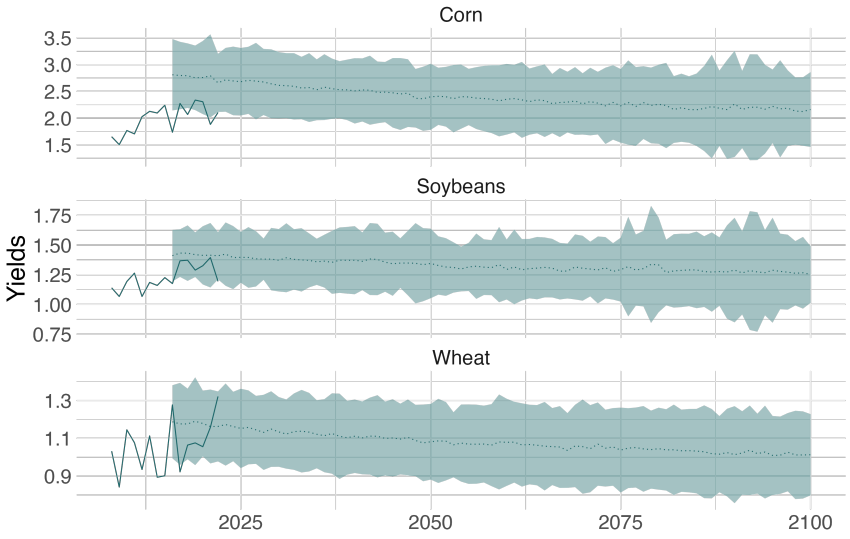
Aggregate U.S. acreage state beliefs. The crop choice problem includes a low-dimensional representation of aggregate U.S. planted acres as a state variable, in the spirit of Krusell and Smith (1998), Weintraub et al. (2008) and Gowrisankaran et al. (2025). Let A_t denote the vector of national planted acres across the four land uses in the model (corn, soybeans, wheat, and other/fallow). I summarize A_t by a discrete *national market state* $s_t \in \{1, \ldots, S\}$ obtained by binning the observed acreage vector into S cells. This discretization is constructed so that farmers can condition on a small number of aggregate states while preserving empirically relevant movements in national acreage.

Farmers form beliefs about the evolution of s_t using a parsimonious autoregressive process for national acres, which I approximate with a Markov transition matrix $\Pi(s'|s)$. This transition matrix enters the expectation in the Bellman equation solved in the NFXP algorithm (Section 5.2).

Figure A15. Fit and projections of country-level yield distributions



(A) United States



(B) Brazil

Notes: The solid line corresponds to country-level average yields for the three considered commodities. The dotted line is the average yields implied by the projections of 29 global circulation models under radiative forcing scenario RCP4.5. The shaded areas are the 0.05-0.95 percentile range. The data was generously shared by Roberto Zuniga.

In estimation, this matrix is treated as observed and estimated from national acreage data.

Country-level yield beliefs. In contrast to county-level yield beliefs, country-level yield beliefs are constructed using a larger ensemble of global climate models. To compute farmers' beliefs on country-level yields, I use the estimated yield-weather response and simulated future weather paths

from the GCMs to project future country-level yield distributions.[32] The procedure proceeds in two steps. First, weather simulations are augmented to account for weather variability. Second, yield variability not explained by the model is added by bootstrapping the residuals of the estimated yield-weather response.

Twenty-nine GCMs provide a path of future weather variables over 2020-2050. The number of simulations in a given year is augmented using a resampling procedure, allowing better capture of within-model weather variability. The resampling procedure uses permutations of weather draws within two years of the considered year. Importantly, this method conserves the matrix of covariance of weather.

A sample of yield predictions is generated using a bootstrap procedure for each given weather path. The procedure samples the residuals at two stages: first, to account for parameter uncertainty, and second, to account for yield variability not explained by the model. This procedure also conserves the cross-sectional correlation of residuals.

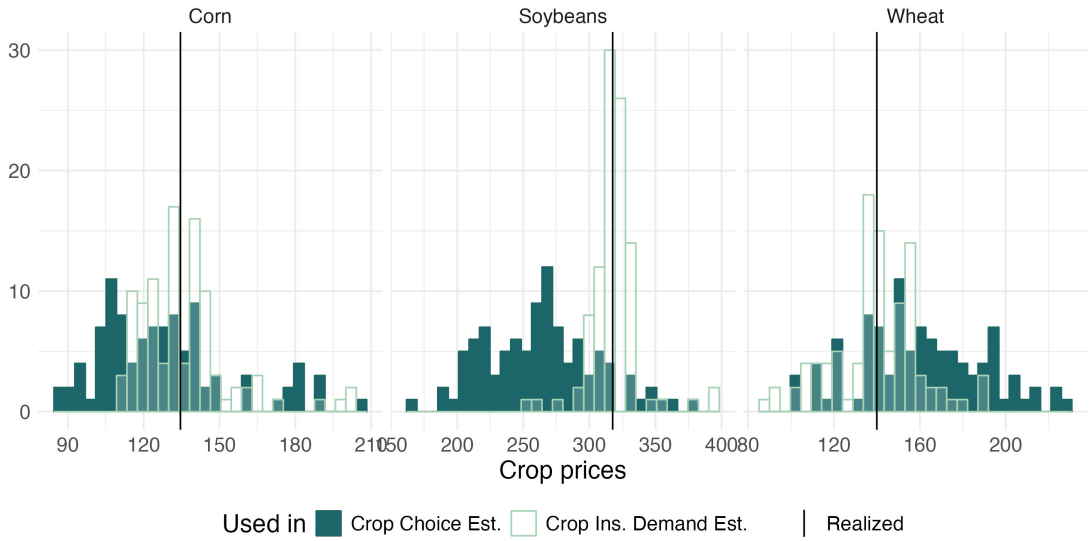
Figure A15 presents the procedure's fit and the time series of the yield projections for two main agricultural producers: the US and Brazil. The model performs well in predicting average yields: the transition between observed data and climate models is seamless. The 0.05-0.95 percentile range covers the pre-2020 observed yield variability.

Crop price beliefs. I combine the estimated crop-demand system (see Section A2) with the country-level yield projections, the endogenous aggregate acreage state, and foreign acreage to derive farmers' crop price beliefs between 2016–2050. These simulated price beliefs reflect (i) climate-driven changes in world yields, (ii) the historical structure of U.S. trade, and (iii) endogenous shifts in U.S. production decisions. They serve as the input to farmers' expectations of revenues and insurance indemnity payments in the simulations that follow.

Crop price beliefs used in the estimation of the crop insurance demand system and those used in the estimation of the dynamic crop choice model are obtained using very different methods. In Figure A16 I compare the resulting distributions in 2016. The two distributions broadly overlap and exhibit similar standard deviations.

[32] Roberto Zuniga generously shared these data.

Figure A16. Crop Price Beliefs — Static versus Dynamic Estimation



Notes: The figures shows 2016 crop price beliefs used in the estimations of the crop insurance demand system (see Section A2) and of the dynamic crop choice model. The vertical lines show the realized crop prices in 2016.

A4.1.3 Premiums

Similar to the procedure in Appendix A3.1.3, I combine farmers' beliefs about yield and crop-price distributions with insurance indemnities formulas (Figure A8) to compute actuarially fair premiums for each county–year–crop–coverage–state s combination. I then apply the status quo subsidies shown in Table A1.

A4.1.4 Inclusive value

The dynamic crop choice model takes as input, for each county m, year t, crop k and state s, the planting-time expected net static profits under the *optimal* crop insurance choice, E^*. This object summarizes the entire insurance block into a single sufficient statistic for the planting decision and is defined in Equation (7) in the main text.

A4.2 NFXP algorithm

Discretized state space and inputs. Let the two-lag crop history be denoted by $(k_{t-2}, k_{t-1}) = (k'', k')$, and let $s \in \{1, \ldots, S\}$ denote the aggregate acreage state. For each county m, year t, crop k, and aggregate state s, the solver takes as inputs: (i) the payoff shifter $\mathbb{E}^*_{kmt}(s)$ (Equation (7)), constructed in Appendix A4.1.4, and (ii) the perceived law of motion for the aggregate state, $\Pi(s'|s)$.

The only stochastic component integrated out in the dynamic-programming step is the i.i.d. type-I extreme value shock ϵ_{ikt}; uncertainty over yields and prices is already integrated into $\mathbb{E}^*_{kmt}(s)$ through the belief objects and insurance block.

Inner loop: backward induction with a terminal continuation value. Fix a candidate parameter vector $\Theta = \{\alpha, \{\phi_{k'',k'\to k}\}_{k'',k',k}\}$. The inner loop computes the expected value function and CCPs over the discretized state space.

Because the environment can be non-stationary over calendar time (through climate change and policy objects), I solve a finite-horizon dynamic program for $t = 1, \ldots, T$ with a terminal continuation value. Let $T = 2050$ denote the terminal year in the horizon used for solution.

Step 0 (terminal condition). I assume that after year T the environment is stationary. I solve the post-terminal stationary problem using $E^*_{mkT}(s)$ and the Markov matrix Π to obtain an ex-ante continuation value $\bar{V}_{k'',k'm,T,s}$ for all k'', k', m, s.

Step 1 (backward recursion). For $t = T-1, \ldots, 1$, compute the conditional values:

$$v_{k'',k'\to k,mts}(\Theta) = \bar{\pi}_{k'',k'\to k,mts} + \delta \Pi(s'|s)\, \bar{V}_{k',km,t+1,s'} \tag{A11}$$

Given $\{v_{k'',k'\to k,mts}(\Theta)\}_k$, the extreme-value assumption implies:

$$\bar{V}_{k'',k'm,t,s}(\Theta) = \text{Euler constant} + \log \sum_k v_{k'',k'\to k,mts}(\Theta) \tag{A12}$$

$$P_{k'',k'\to k,mts}(\Theta) = \frac{\exp\left(v_{k'',k'\to k,mts}(\Theta)\right)}{\sum_k \exp\left(v_{k'',k'\to k,mts}(\Theta)\right)} \tag{A13}$$

Outer loop: likelihood maximization. Let $N_{k'',k'\to k,mt}$ denote the (area-weighted) number of parcels in county m, year t, with history k'', k' that choose crop k. The log-likelihood is

$$\ell(\Theta) = \sum_{m,t,k'',k'} \sum_k N_{k'',k'\to k,mt} \log P_{k'',k'\to k,mt}(\Theta). \tag{A14}$$

The NFXP outer loop maximizes (A14). Each evaluation of $\ell(\Theta)$ calls the inner loop described above to compute CCPs consistent with Θ.

A4.3 Dynamic Estimation Results

Robustness Table A10 reports a robustness check that re-estimates the model after restricting the estimation sample to years prior to 2018. In later years, CDL classification uses information from prior-year classifications in its training pipeline, which may mechanically increase persistence in observed land-use transitions. Re-estimating the model on the pre-2018 subsample yields parameter estimates that are qualitatively similar to the baseline, indicating that the estimated degree of state dependence and the implied transition costs are not driven by potential changes in CDL classification methodology.

Land use elasticities. To quantify acreage responses to changes in crop-insurance incentives, I compute long-run elasticities of planted acres with respect to premium subsidy exposure. Specifically, I solve the model under the status quo and under counterfactual subsidy schedules that permanently scale subsidy exposure by 10% either for all crops or for a single crop holding other crops fixed. Section 6 outlines the equilibrium concept.

For each scenario, I construct a county–crop dollar-based exposure measure by combining the statutory subsidy rate with equilibrium take-up and expected indemnities:

$$S^{\$}_{mkt} = \mathbb{E}_j\left[\text{subsidy}^k_j \cdot \text{Premium}^k_{jmt} \cdot \sigma^k_{jmt}\right].$$

I then average acres and exposures over 2020–2050 and aggregate across counties to obtain baseline and counterfactual totals (A_0, A_1) and (S_0, S_1) for each crop.

Elasticities are reported as arc elasticities, $\varepsilon = \frac{(A_1 - A_0)/\left(\frac{A_1+A_0}{2}\right)}{(S_1 - S_0)/\left(\frac{S_1+S_0}{2}\right)}$. For crop-specific shocks, I additionally report cross elasticities by dividing each crop's acreage response by the shocked crop's exposure change.

Under a permanent proportional 10% increase in premium-subsidy exposure for all crops and coverage levels, the long-run elasticities with respect to premium-subsidy dollars are 0.009 for corn, and 0.015 for both soybeans and wheat, with an aggregate elasticity of 0.012, implying a roughly 0.12% increase in total cultivated acres. When exposure is increased for a single crop holding other crops' subsidy schedules fixed, the own-exposure elasticities are 0.007 for corn, 0.015 for soybeans, and 0.024 for wheat, while cross-crop effects are approximately an order of magnitude smaller. Notably, cross elasticities between corn and soybeans are positive, consistent with these crops being com-

monly produced within the same rotational system so that policies favoring one crop can increase the profitability of that bundle and expand acreage of both crops. In contrast, cross elasticities involving wheat are negative, consistent with wheat competing for land with corn and soybeans rather than being part of the same rotational bundle.

These elasticities are smaller than the county–crop estimates in Yu et al. (2018), who find that a 10% increase in premium subsidies raises a crop's planted acreage by about 0.43% holding competing subsidies fixed, but they are in line with earlier evidence of more modest acreage responses to crop insurance subsidies and participation (Young et al., 2001; Goodwin et al., 2004). Because premium subsidies are a small share of expected per-acre returns, these acreage elasticities with respect to subsidy dollars imply economically meaningful elasticities with respect to overall expected returns (roughly 0.2–0.3 when scaled by typical subsidy shares), broadly consistent with dynamic land-use estimates such as the long-run cropland–price elasticity of about 0.3 reported by Scott (2014).

Model fit. I assess the fit of the dynamic crop choice model by comparing model-implied conditional choice probabilities (CCPs) to CCPs measured in the data (see Section 3.4 for construction details). Using the counterfactual algorithm described in Section 6, I compute equilibrium CCPs in 2021 under the status quo subsidy schedule. Climate evolves as projected by six GCMs under scenario RCP4.5 (see Section A4.1.1). Figure A17 plots binscatter regressions of model-implied CCPs against their data counterparts, separately by action. The model reproduces the broad cross-sectional variation in planting probabilities across counties and crop histories: model-implied CCPs are strongly positively related to the ground-truth CCPs inferred from the Cropland Data Layer. The pooled slope is 0.61 ($R^2 = 0.43$), and action-specific slopes range from 0.52 (soybeans) to 0.83 (fallow/other), with R^2 between 0.25 (wheat) and 0.67 (fallow/other).

Table A10. Dynamic crop choice estimates — Robustness

Parameter	Full Sample	Year < 2018
$\hat{\alpha}$	0.001038	0.001088
$\phi_{\text{Corn-Corn}\to\text{Corn}}$	2326	1966
$\phi_{\text{Corn-Corn}\to\text{Soybeans}}$	1550	1294
$\phi_{\text{Corn-Corn}\to\text{Wheat}}$	695	437
$\phi_{\text{Corn-Fallow}\to\text{Corn}}$	420	369
$\phi_{\text{Corn-Fallow}\to\text{Soybeans}}$	-203	103
$\phi_{\text{Corn-Fallow}\to\text{Wheat}}$	779	983
$\phi_{\text{Corn-Soybeans}\to\text{Corn}}$	2761	2350
$\phi_{\text{Corn-Soybeans}\to\text{Soybeans}}$	1696	1297
$\phi_{\text{Corn-Soybeans}\to\text{Wheat}}$	889	546
$\phi_{\text{Corn-Wheat}\to\text{Corn}}$	2124	1752
$\phi_{\text{Corn-Wheat}\to\text{Soybeans}}$	-161	-425
$\phi_{\text{Corn-Wheat}\to\text{Wheat}}$	1119	901
$\phi_{\text{Fallow-Corn}\to\text{Corn}}$	-1563	-1012
$\phi_{\text{Fallow-Corn}\to\text{Soybeans}}$	-1218	-473
$\phi_{\text{Fallow-Corn}\to\text{Wheat}}$	-1889	-1712
$\phi_{\text{Fallow-Fallow}\to\text{Corn}}$	-5201	-5046
$\phi_{\text{Fallow-Fallow}\to\text{Soybeans}}$	-4720	-4822
$\phi_{\text{Fallow-Fallow}\to\text{Wheat}}$	-4608	-4458
$\phi_{\text{Fallow-Soybeans}\to\text{Corn}}$	-1683	-624
$\phi_{\text{Fallow-Soybeans}\to\text{Soybeans}}$	-752	-177
$\phi_{\text{Fallow-Soybeans}\to\text{Wheat}}$	-2161	-1544
$\phi_{\text{Fallow-Wheat}\to\text{Corn}}$	-532	-221
$\phi_{\text{Fallow-Wheat}\to\text{Soybeans}}$	-3159	-2822
$\phi_{\text{Fallow-Wheat}\to\text{Wheat}}$	-707	-681
$\phi_{\text{Soybeans-Corn}\to\text{Corn}}$	998	514
$\phi_{\text{Soybeans-Corn}\to\text{Soybeans}}$	2674	2195
$\phi_{\text{Soybeans-Corn}\to\text{Wheat}}$	-687	-1032
$\phi_{\text{Soybeans-Fallow}\to\text{Corn}}$	-770	-274
$\phi_{\text{Soybeans-Fallow}\to\text{Soybeans}}$	743	803
$\phi_{\text{Soybeans-Fallow}\to\text{Wheat}}$	-1798	-906

Continued on next page

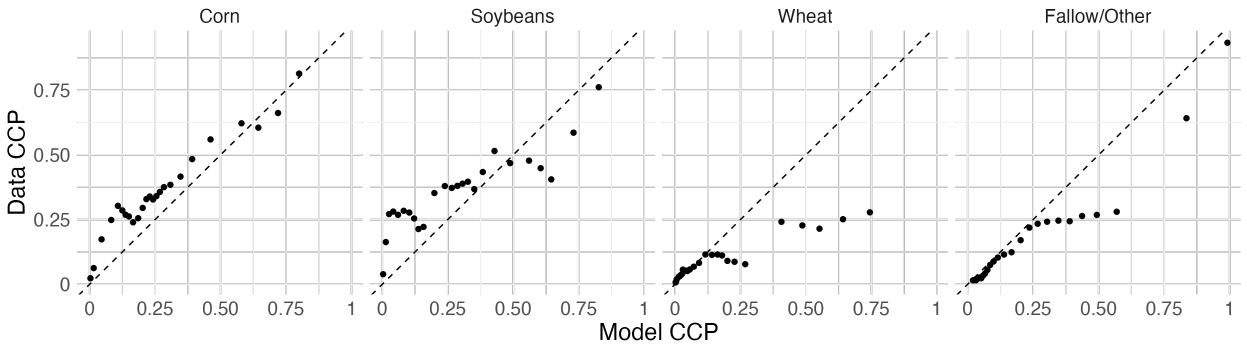
Parameter	Full Sample	Year < 2018
$\phi_{\text{Soybeans-Soybeans}\rightarrow\text{Corn}}$	1149	807
$\phi_{\text{Soybeans-Soybeans}\rightarrow\text{Soybeans}}$	2511	2055
$\phi_{\text{Soybeans-Soybeans}\rightarrow\text{Wheat}}$	965	645
$\phi_{\text{Soybeans-Wheat}\rightarrow\text{Corn}}$	2316	1724
$\phi_{\text{Soybeans-Wheat}\rightarrow\text{Soybeans}}$	2434	2024
$\phi_{\text{Soybeans-Wheat}\rightarrow\text{Wheat}}$	1030	788
$\phi_{\text{Wheat-Corn}\rightarrow\text{Corn}}$	-702	-557
$\phi_{\text{Wheat-Corn}\rightarrow\text{Soybeans}}$	-187	-134
$\phi_{\text{Wheat-Corn}\rightarrow\text{Wheat}}$	786	657
$\phi_{\text{Wheat-Fallow}\rightarrow\text{Corn}}$	-2144	-2139
$\phi_{\text{Wheat-Fallow}\rightarrow\text{Soybeans}}$	-2239	-1909
$\phi_{\text{Wheat-Fallow}\rightarrow\text{Wheat}}$	1326	1211
$\phi_{\text{Wheat-Soybeans}\rightarrow\text{Corn}}$	-127	-176
$\phi_{\text{Wheat-Soybeans}\rightarrow\text{Soybeans}}$	1349	1209
$\phi_{\text{Wheat-Soybeans}\rightarrow\text{Wheat}}$	2042	1988
$\phi_{\text{Wheat-Wheat}\rightarrow\text{Corn}}$	629	567
$\phi_{\text{Wheat-Wheat}\rightarrow\text{Soybeans}}$	-316	-217
$\phi_{\text{Wheat-Wheat}\rightarrow\text{Wheat}}$	2218	2178

Table A11. Long-run acreage elasticities with respect to premium-subsidy exposure

Scenario:	All crops +10%	Corn +10%	Soybeans +10%	Wheat +10%
All crops	0.0124	0.0031	0.0079	6e-04
Corn	0.0091	0.0066	0.0045	-8e-04
Soybeans	0.015	0.0014	0.0153	-0.0044
Wheat	0.0148	-0.0031	-0.0072	0.0237

Notes: Entries report arc elasticities of acres with respect to premium-subsidy exposure (dollar-based), computed by comparing the stationary equilibrium under the status quo to a permanent +10% shift in exposure. Columns correspond to the shocked crop(s); rows correspond to acreage responses by crop.

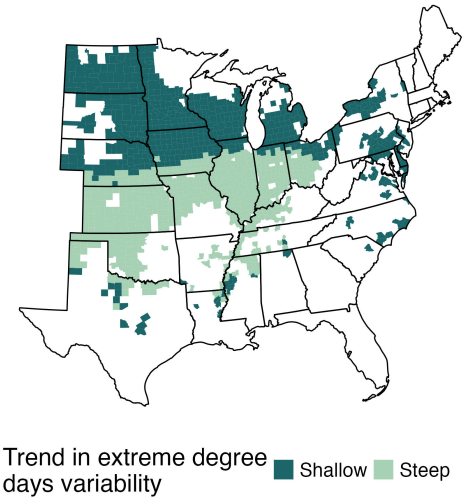
Figure A17. Dynamic model fit



Notes: The figure presents binscatter regressions of model-implied CCPs on ground-truth CCPs for 2021, separately by possible action (corn, soybeans, wheat, fallow). Data on CCPs are obtained using the CropLand Data Layer (Section 3.4). I stack all CCP across all states (land use in the past two years).

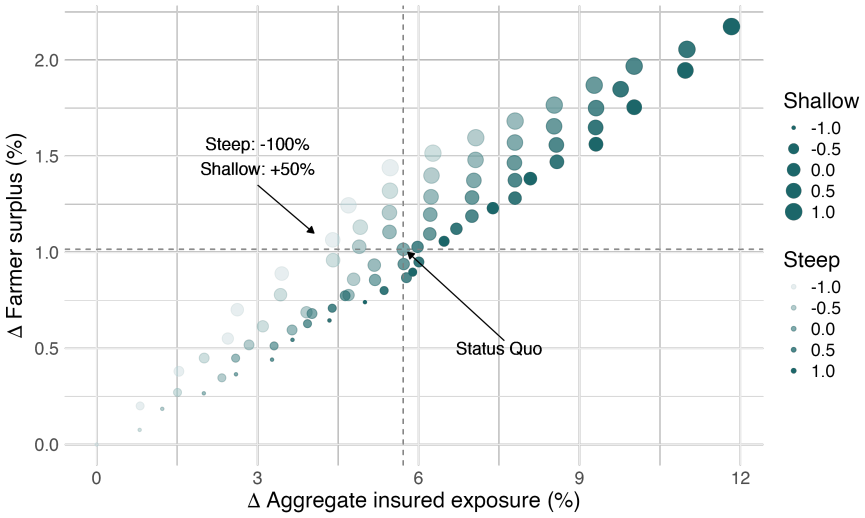
A5 Supplemental Material: Counterfactual Results

Figure A18. Regional Classification Used for Targeted Subsidies

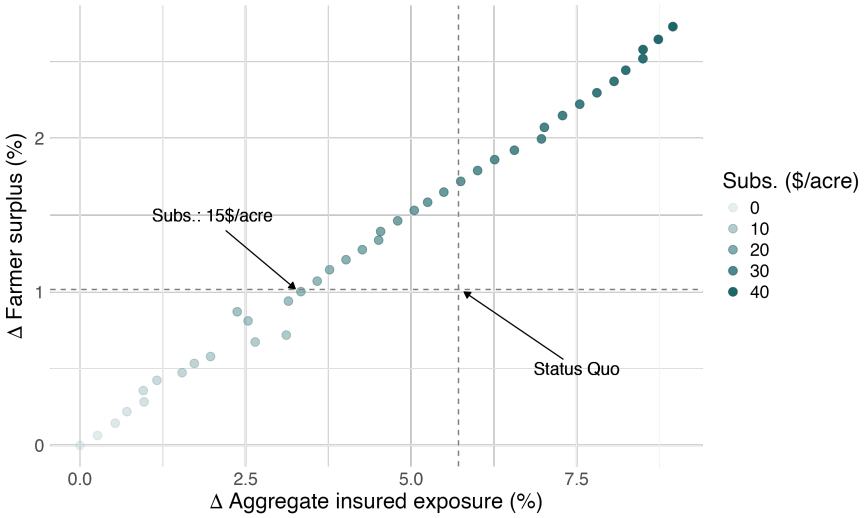


Notes: The map shows the regional classification used in the *By Region* subsidy counterfactuals. Counties are grouped according to the trend in the variability of extreme degree days during the growing season. The trend is estimated by regressing the county-level standard deviation of extreme degree days on time using simulated weather paths from the climate projections described in Appendix A4. Counties with trends above the sample median are classified as having *steep* increases in climate risk, while counties below the median are classified as having *shallow* trends. This classification determines how subsidies are adjusted under the *By Region* policy: subsidy generosity is reduced in counties experiencing steeper increases in climate risk and increased in counties where risk trends are flatter. The map therefore defines the regional groups used to implement the targeting rules analyzed in Section 6.

Figure A19. Welfare and Insurance Exposure under Alternative Subsidy Designs



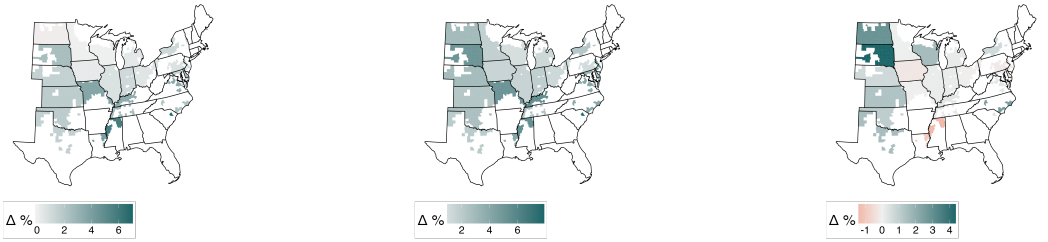
(A) By Region



(B) Unconditional

Notes: The figure compares equilibrium outcomes under alternative crop insurance subsidy schedules over the period 2030–2050. The horizontal axis reports the percent change in aggregate insured exposure relative to the no-subsidy counterfactual, measured in acre-equivalent units. The vertical axis reports the percent change in farmer surplus relative to the no-subsidy counterfactual. Dashed lines indicate the status quo aggregate outcomes. Panel (A) considers subsidy schedules that remain tied to actuarial risk but vary by regional climate trends. The marker size and shading index the subsidy adjustment applied to counties in regions with shallow and steep climate-risk trends. The annotated policy reduces subsidies in counties with steep increases in climate risk and raises them in counties with shallow trends. Panel (B) considers unconditional subsidies that take the form of per-acre payments conditional on insurance purchase and do not vary with actuarial risk. Marker size and shading indicate the level of the unconditional payment in dollars per acre. The annotated point corresponds to a subsidy of $15 per acre. Points to the upper left of the status quo deliver higher farmer surplus with lower aggregate insured exposure, indicating that they improve on the status quo while reducing the extent of insurance-induced exposure.

Figure A20. Land Use across Space



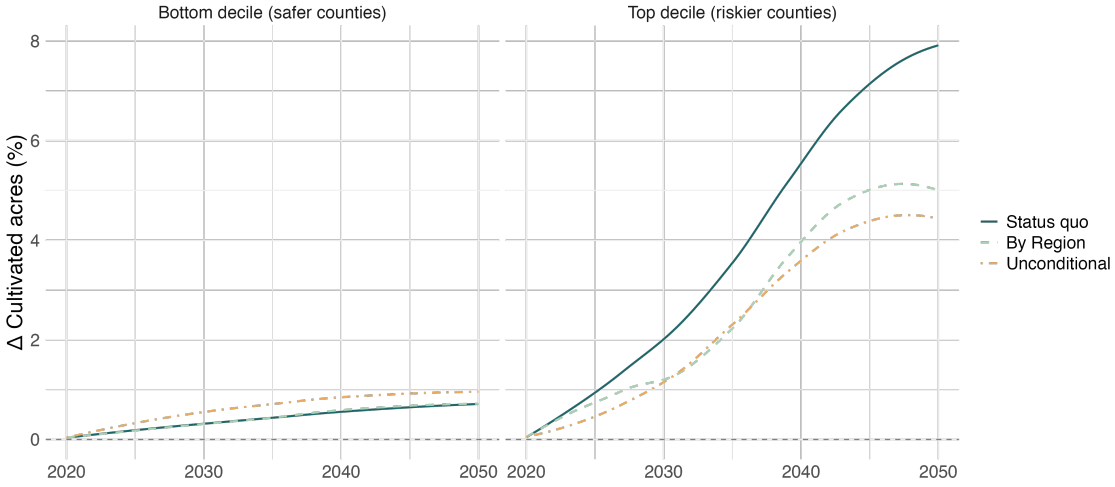
(A) Status Quo - Corn **(B)** Status Quo - Soybeans **(C)** Status Quo - Wheat

(D) By Region - Corn **(E)** By Region - Soybeans **(F)** By Region - Wheat

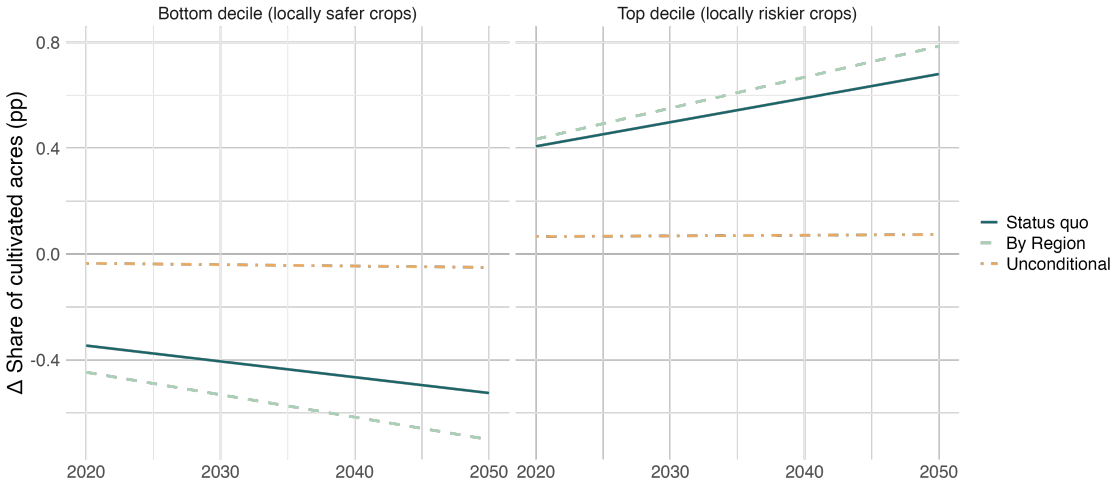
(G) Unconditional - Corn **(H)** Unconditional - Soybeans **(I)** Unconditional - Wheat

Notes: The maps show the spatial distribution of the average change in crop acreage over the period 2030–2050 relative to the no-subsidy counterfactual. Positive values indicate counties where the policy increases acreage planted in the corresponding crop, while negative values indicate reductions. The first row reports outcomes under the status quo subsidy schedule, where subsidies are proportional to actuarially fair premiums. The second row reports outcomes under the "By Region" policy, where subsidy generosity varies with local trends in climate risk. The third row reports outcomes under the "Unconditional" policy, where subsidies take the form of lump-sum payments conditional on purchasing insurance and do not depend on actuarial risk.

Figure A21. Crop Insurance Subsidies Induced Land Use Distortions Over Time



(A) Across counties



(B) Within county

Notes: The figure shows how the land-use distortions induced by crop insurance subsidies evolve over time under alternative subsidy designs. In the "Status Quo" scenario, subsidies are proportional to actuarially fair premiums. In the "By Region" scenario, subsidies remain proportional to premiums, but their generosity varies with the local trend in climate risk. In the "Unconditional" scenario, subsidies take the form of lump-sum payments conditional on insurance purchase and do not depend on actuarial risk. Panel (A) focuses on distortions across counties. Counties are ranked each year by their average expected indemnities, which summarize local production risk, and the figure reports the weighted average change in cultivated acreage relative to the no-subsidy counterfactual for counties in the bottom and top deciles of that distribution. Panel (B) focuses on distortions within counties across crops. Within each county-year, crops are ranked by expected indemnities relative to the county-year average, and the figure reports the weighted average change in crop shares, relative to the no-subsidy counterfactual, for crops in the bottom and top deciles of that within-county distribution.

References for Online Appendix

Adjemian, M. K. and A. Smith (2012): "Using USDA forecasts to estimate the price flexibility of demand for agricultural commodities," *American Journal of Agricultural Economics*, 94, 978–995.

Annan, F. and W. Schlenker (2015): "Federal crop insurance and the disincentive to adapt to extreme heat," *American Economic Review*, 105, 262–266.

Athey, S., J. Tibshirani, and S. Wager (2019): "Generalized random forests," *The Annals of Statistics*, 47, 1148 – 1178.

Goodwin, B. K., M. L. Vandeveer, and J. L. Deal (2004): "An empirical analysis of acreage effects of participation in the federal crop insurance program," *American Journal of Agricultural Economics*, 86, 1058–1077.

Gowrisankaran, G., A. Langer, and W. Zhang (2025): "Policy uncertainty in the market for coal electricity: The case of air toxics standards," *Journal of Political Economy*.

Harwood, J., R. Heifner, K. H. Coble, J. Perry, and A. Somwaru (1999): "Measuring Price and Yield Risk," in *Managing Risk in Farming: Concepts, Research, and Analysis*, U.S. Department of Agriculture, Economic Research Service, no. 774 in Agricultural Economic Report.

Havnes, T. and M. Mogstad (2011): "No child left behind: Subsidized child care and children's long-run outcomes," *American Economic Journal: Economic Policy*, 3, 97–129.

Krusell, P. and A. A. Smith, Jr (1998): "Income and wealth heterogeneity in the macroeconomy," *Journal of political Economy*, 106, 867–896.

RMA, U. R. M. A. (2023): "Summary of Business," Accessed: 10 May 2023.

Roberts, M. J. and W. Schlenker (2013): "Identifying supply and demand elasticities of agricultural commodities: Implications for the US ethanol mandate," *American Economic Review*, 103, 2265–2295.

Rust, J. (1987): "Optimal replacement of GMC bus engines: An empirical model of Harold Zurcher," *Econometrica: Journal of the Econometric Society*, 999–1033.

Scott, P. (2014): "Dynamic discrete choice estimation of agricultural land use," Working Paper.

Soil Survey Staff, Natural Resources Conservation Service, U. S. D. o. A. (2024): "Web Soil Survey," Accessed 10 February 2024.

Weintraub, G. Y., C. L. Benkard, and B. Van Roy (2008): "Markov perfect industry dynamics with many firms," *Econometrica*, 76, 1375–1411.

Young, C. E., M. L. Vandeveer, and R. D. Schnepf (2001): "Production and price impacts of US crop insurance programs," *American Journal of Agricultural Economics*, 83, 1196–1203.

Yu, J., A. Smith, and D. A. Sumner (2018): "Effects of crop insurance premium subsidies on crop acreage," *American Journal of Agricultural Economics*, 100, 91–114.